Artificial Intelligence in magnetic Resonance guided Radiotherapy : medical and physical considerations on state of art and future perspectives

Artificial Intelligence in Magnetic Resonance guided Radiotherapy: medical and physical considerations on state of art and future perspectives

Davide Cusumano [1], Luca Boldrini [1], Jennifer Dhont [2], Claudio Fiorino [3], Olga Green [4], Görkem Güngör [5], Núria Jornet [6], Sebastian Klüter [7], Guillaume Landry [8], Gian Carlo Mattiucci [1], Lorenzo Placidi [9], Nick Reynaert [10], Ruggero Ruggieri [11], Stephanie Tanadini-Lang [12], Daniela Thorwarth [13], Poonam Yadav [14], Yingli Yang [15], Vincenzo Valentini [1], Dirk Verellen [16], Luca Indovina [1]

Affiliations

- [1] Fondazione Policlinico Universitario Agostino Gemelli, IRCCS, Rome, Italy.
- [2] Maastro Clinic, Maastrict, the Netherlands.
- [3] Medical Physics, San Raffaele Scientific Institute, Milan, Italy.
- [4] Department of Radiation Oncology, Washington University School of Medicine, St. Louis, MO, USA.
- [5] Acıbadem MAA University, School of Medicine, Department of Radiation Oncology, Maslak Istanbul, Turkey.
- [6] Servei de Radiofísica i Radioprotecció, Hospital de la Santa Creu i Sant Pau, Spain.
- [7] Department of Radiation Oncology, Heidelberg University Hospital, Heidelberg, Germany.
- [8] Department of Radiation Oncology, LMU Munich, Munich, Germany; German Cancer Consortium (DKTK), Munich, Germany.
- [9] Fondazione Policlinico Universitario Agostino Gemelli, IRCCS, Rome, Italy. Electronic address: lorenzo.placidi@policlinicogemelli.it.
- [10] Department of Medical Physics, Institut Jules Bordet, Belgium.
- [11] Dipartimento di Radioterapia Oncologica Avanzata, IRCCS "Sacro cuore - don Calabria", Negrar di Valpolicella (VR), Italy.
- [12] Department of Radiation Oncology, University Hospital Zurich and University of Zurich, Zurich, Switzerland.
- [13] Section for Biomedical Physics, Department of Radiation Oncology, University Hospital Tüebingen, Tübingen, Germany.
- [14] Department of Human Oncology School of Medicine and Public Heath University of Wisconsin - Madison, USA.

- **[15] Department of Radiation Oncology, David Geffen School of Medicine, University of California Los Angeles, USA.**
- **[16] Department of Medical Physics, Iridium Cancer Network, Belgium; Faculty of Medicine and Health Sciences, Antwerp University, Antwerp, Belgium.**

Abstract

Over the last years, technological innovation in Radiotherapy (RT) led to the introduction of Magnetic Resonance-guided RT (MRgRT) systems.

Due to the higher soft tissue contrast compared to on-board CT-based systems, MRgRT is expected to significantly improve the treatment in many situations. MRgRT systems may extend the management of inter- and intra-fraction anatomical changes, offering the possibility of online adaptation of the dose distribution according to daily patient anatomy and to directly monitor tumor motion during treatment delivery by means of a continuous cine MR acquisition.

Online adaptive treatments require a multidisciplinary and well-trained team, able to perform a series of operations in a safe, precise and fast manner while the patient is waiting on the treatment couch.

Artificial Intelligence (AI) is expected to rapidly contribute to MRgRT, primarily by safely and efficiently automatising the various manual operations characterizing online adaptive treatments. Furthermore, AI is finding relevant applications in MRgRT in the fields of image segmentation, synthetic CT reconstruction, automatic (on-line) planning and the development of predictive models based on daily MRI.

This review provides a comprehensive overview of the current AI integration in MRgRT from a medical physicist's perspective. Medical physicists are expected to be major actors in solving new tasks and in taking new responsibilities: their traditional role of guardians of the new technology implementation will change with increasing emphasis on the managing of AI tools, processes and advanced systems for imaging and data analysis, gradually replacing many repetitive manual tasks.

Keywords: Artificial Intelligence, Deep Learning, MR-guided Radiotherapy, Online Adaptive Radiotherapy, MR-Linac

1. Background

In recent years, the development of artificial intelligence (AI) started to change the world we live in, bringing innovations in social life, technology and health care that were unimaginable a decade ago. Especially the fast growing utilization of deep learning (DL) methods has enabled breakthroughs in multiple applications [1]. In radiotherapy (RT), AI has already proven to be a valuable tool to support oncological workflows, providing significant improvements in many steps of patient care from diagnosis to treatment delivery [2,3].

At the heart of the expansion of AI is the current exponential growth of the amount of available information in digital format. For the same reason, there is great potential for a widespread use of AI in RT, a highly computerized medical speciality, including digital diagnostic and positioning imaging data, treatment plans, treatment delivery records, follow-up imaging, as well as clinical and molecular data [4].

A considerable amount of this potential lies within the area of image and data processing: as an example, it is nowadays possible to train an artificial neural network (NN) to automatically perform specific tasks that are currently carried out manually, or to predict the outcome or associated toxicity of a therapeutic treatment in advance, guiding treatment decisions [5,6]. Given the amount and variety of available data, the number of implemented and foreseeable applications is hard to estimate [2,4].

However, the advent of AI in radiation oncology (RO) and its fruitful and correct implementation also represents a major challenge, requiring both vision and guidance, as well as major changes in tasks and responsibilities of all the actors of the radiotherapy chain, including medical physicists [7,8]. Modern RT has always been inextricably linked to technological innovation, and has benefitted from continuous development of increasingly advanced and complex image-guided radiotherapy (IGRT) systems, resulting in amazing advancements in treatment delivery accuracy [9,10].

MR-guided radiotherapy (MRgRT) systems represent one of the latest frontiers of technological innovation, combining a linear accelerator (Linac) with an on-board magnetic resonance (MR) imaging system.

While the clinical introduction of these systems was only a few years ago, promising clinical benefits already emerged, promising to represent a major step forward in the clinical management of several tumour types [11–14]. To date, two commercial MRgRT systems are in clinical use, mainly differing in the magnetic field (B) strength of the on-board MR scanner: MRIdian Linac (ViewRay, Mountain View, California, USA) joins a 6 MV Flattening Filter Free (FFF) Linac with a 0.35 T MR imaging system, while Unity (Elekta,

Stockholm, Sweden) mounts a 7 MV FFF Linac combined to a 1.5 T MR scanner [15,16]. An example of MR images obtained using these hybrid systems is illustrated in Figure 1.

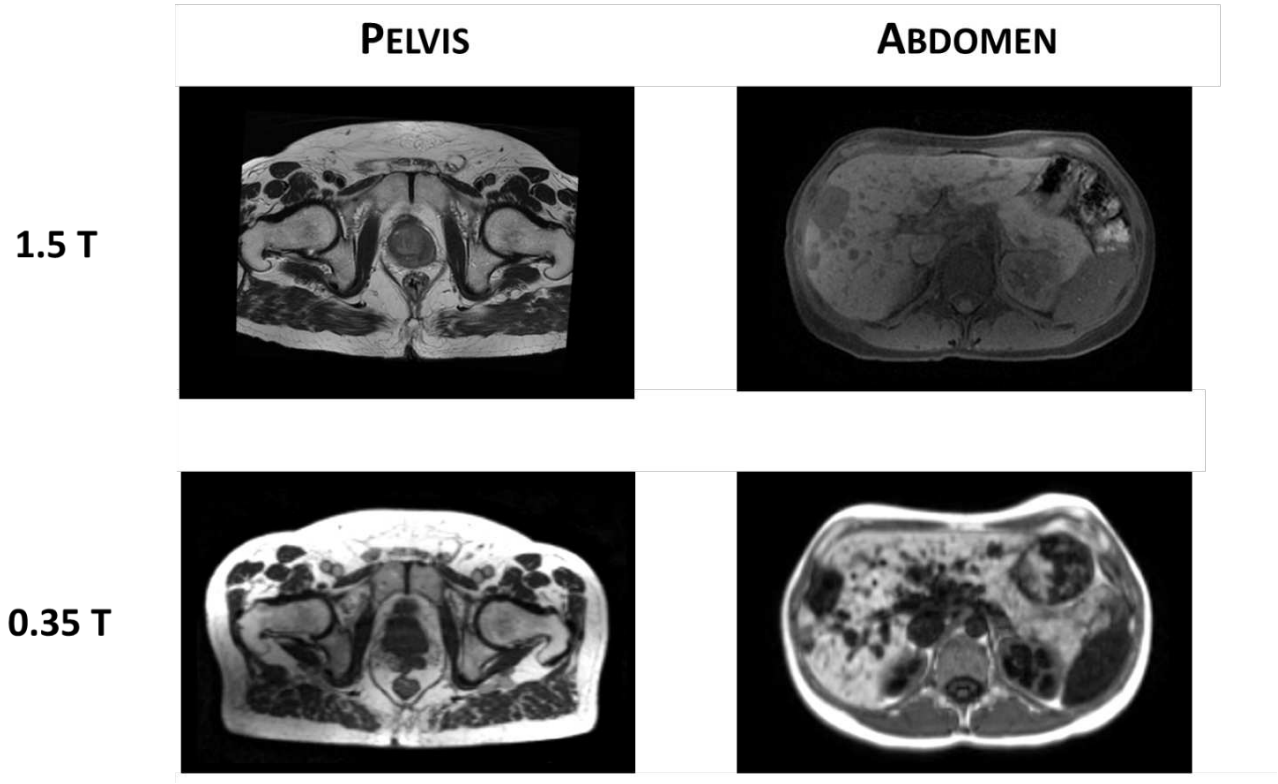

Figure 1 - Example of MR images acquired using hybrid machines for a pelvic case (left) and an abdominal case (right): in the upper part two examples of MR images acquired using 1.5 T on-board MR scanner (T2-weighted MRI for pelvis and T1-weighted with fat suppression for the abdomen).In the lower part, two MR images acquired using a 0.35 T MR scanner (TRUFI acquisition for pelvic case and T1 weighted with navigator for the abdominal case)

On-board MR imaging (MRI) offers higher soft tissue contrast compared to standard imaging modalities such as Cone Beam Computed Tomography (CBCT), resulting in better visualization of anatomy and a significant reduction in contouring and patient positioning uncertainties [17]. Furthermore, using techniques like diffusion-weighted MRI, dynamic contrast enhanced (DCE) MRI or T1 and T2 mapping, MR facilitates multi-parametric quantitative imaging that is expected to enable more personalized treatment ~~concepts~~ approaches [18,19]. Another important advantage is the possibility of directly monitoring tumour motion during RT delivery by means of continuous and non-invasive cine-MR acquisition. Currently, this can be performed with 4-8 frames per second in a single sagittal plane or 5 frames per second in three orthogonal planes, depending on the technology used [20,21].

In addition to advanced intra-fraction motion management, MRgRT technology offers the possibility to online adapt the treatment plan based on the patient's daily anatomy, allowing effective management of inter-fraction variations that may occur over the course of the treatment [22,23].

Figure 2 reports an example of inter-fraction variation that may occurred during an abdominal MRgRT treatment of five fractions.

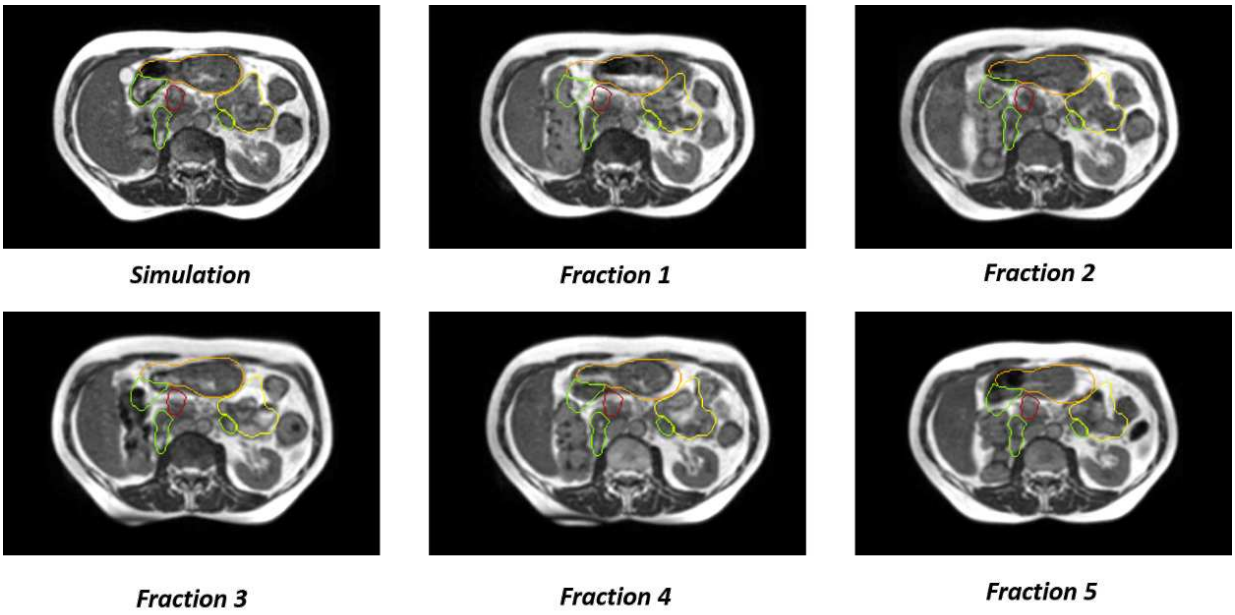

Figure 2 - Example of inter-fraction variability during a five fraction MRgRT treatment of a patient affected by pancreatic cancer. The following contours from the day of simulation are projected onto the fraction: GTV (red), duodenum (green), stomach (orange) and bowel bag (yellow)

This procedure, often requiring a multi-disciplinary and highly qualified team and executed while the patient stays in treatment position, is known as online adaptive MRgRT: to date, it is performed mainly manually, requiring long execution times and tight manual checklists, as many of the single workflow steps are subject to human error [23–25]. With daily pre-treatment MRI, additional functional imaging and in-treatment cine-MRI, a huge amount of information is available, often overwhelming human capabilities. Therefore, AI-driven image analysis and predictive models can be a powerful tool in optimally exploiting this patient-specific information. Furthermore, there is a strong need for automation of manual processes in online adaptive treatments, as they currently have a significant impact on treatment time and as such impact on an efficient use of this technology [26,27].

The aim of this work is to provide a comprehensive overview of the current integration of AI in the field of MRgRT from a medical physics perspective. The objective is to show what is already applied in clinical

practice and what is under development, as well as to highlight what is expected in the next years aiming to increase treatment efficiency and improve personalisation of MRgRT treatments.

2. Materials and Methods

The work has been divided into six sections, covering the main areas of AI applications in MRgRT (see Figure 3): for each section, a dedicated literature analysis was carried out with the aim of providing an overview of the current scientific activity in each field.

In some of the investigated areas (synthetic CT (sCT) generation, autosegmentation, 3D motion management and predictive modelling), several MRgRT-related studies have been published, preluding a possible clinical implementation in the near future. In other areas, such as automation in planning and QA, only a few MRgRT-specific experiences have been reported so far, but it is to be expected that they will play a significant role in the coming years.

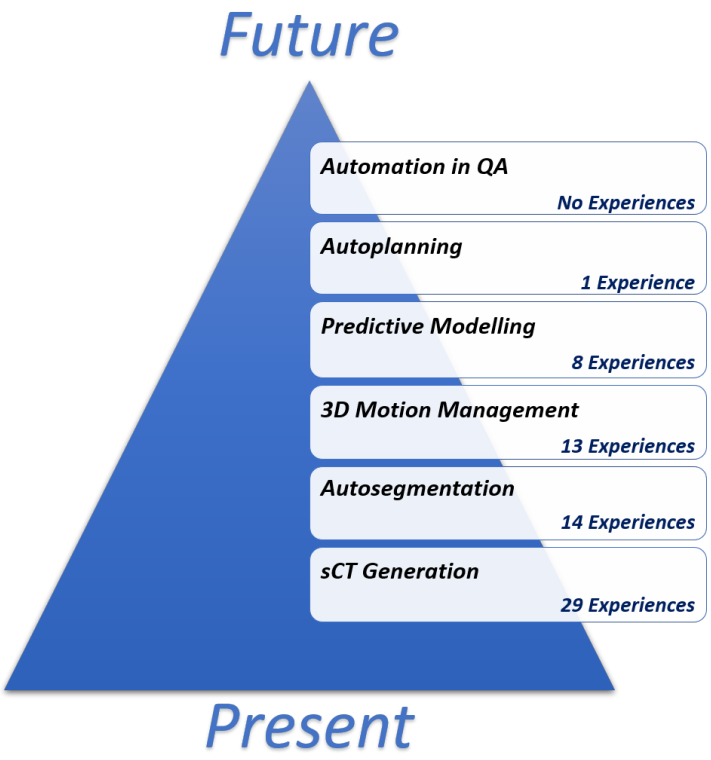

Figure 3- Number of AI-based experiences in MRgRT field according to Scopus database in December 2020

A literature search was performed in the Scopus database considering December 2020 as last update and combining four general key-title words ("*MR-guided Radiotherapy*" OR "*MRgRT*" AND "*Deep Learning*" OR "*Artificial Intelligence*") with specific key words for each section. A summary of the keywords is

reported in Table 1 of supplementary materials. Only original papers written in English language were considered in the literature analysis. In addition, inclusion criteria were defined for each topic, with the aim of focusing on experiences related to AI in MRgRT. A comprehensive list of inclusion and exclusion criteria for each section is reported in Table 2 of supplementary materials.

The review concludes with a final paragraph where the expected clinical benefits for the patient and the main ethical issues related to AI integration in MRgRT are presented and discussed.

3. **Synthetic CT generation**

To date, the clinical workflow of MRgRT generally requires a two-step simulation, consisting of an MR acquisition on the hybrid machine followed by a CT acquisition. Important to note is that the two procedures have to be executed with the patient in the same treatment position and within a short time interval to minimize anatomical changes as much as possible [11,22].

The CT image acquisition is a mandatory step in the current workflow, as it provides the electron density (ED) map on the basis of which the dose distribution is calculated. The simulation MR image is needed for contouring of the target volume and the organs at risk (OARs) as well as a reference image for patient setup.

On low field MRgRT systems the ED map is usually derived by fusing the acquired CT image with the simulation MRI by means of deformable image registration. Such procedures are repeated during the online adaptive treatment and possible differences in terms of air bubbles or body shape are compensated by means of dedicated structures with assigned bulk ED values [28,29].

On high field MRgRT systems, the ED map is usually obtained by rigidly registering the planning CT during simulation and then assigning bulk ED values during online adaptive treatments [30].

Both strategies can lead to suboptimal results during online adaptive procedures, especially in the presence of hollow OARs (such as bowel, stomach, rectum), where the different filling status can lead to large changes in the ED map, reflecting a significant inter-fraction variability [11,31].

An accurate ED map assignment is a crucial aspect in RT in general to have a good estimation of the dose but is even more crucial in MRgRT treatments. The dose distribution is influenced by the presence of the magnetic field and non-negligible effects may occur when the radiation beams pass through tissue inhomogeneities, both in the presence of low and high magnetic fields [32,33].

In this context, the idea of removing the CT acquisition from the MRgRT clinical workflow using an AI-based system able to generate a synthetic CT (sCT) image from the acquired MRI has grown in recent years, with several research groups already demonstrating its feasibility on both low and high field MRI [34–36]. The idea of implementing an MR-only RT workflow would bring considerable benefits in daily clinical practice. First, it would significantly simplify the clinical workflow, making it more rapid and efficient and opening the possibility of treating the patient in the same simulation session, carrying significant advantages especially in case of patients requiring urgent palliative care or patients in pain [37].

The use of sCT generated from daily MRI would also remove the uncertainties due to CT-MR image registration and would save the patient additional exposure to ionizing radiation, ensuring that the only dose delivered to the patient is the one needed for treatment purposes [38,39].

The idea of removing the CT acquisition from a clinical RT workflow is antecedent to the advent of MR-Linac systems, as demonstrated by different experiences reporting the idea of performing the treatment planning directly on MR images acquired using an external MR scanner or a MR simulator [40,41].

The advantages offered by the MR-only RT workflow in terms of enhancement of image quality and reduction of imaging exposure are also valid if the RT treatment is planned on MRI and then delivered on conventional CBCT-based linac systems. For these reasons, several attempts have been made even before the introduction of AI to allow for treatment planning directly on MR images, mostly by generating ED maps starting from an atlas or using bulk approaches, consisting of segmenting the MR image in a fixed number of density levels (i.e. air, lung, fat, soft-tissue and bone) and assigning an ED bulk value to each level of segmentation [42,43]. Through these strategies, sufficiently good dose accuracy was reported, even in the presence of a magnetic field. A comprehensive analysis of the performance achievable using these methods can be found in several reviews on this topic [40,44,45]. The main disadvantage of these methods is that they are time consuming, making them difficult to use in online adaptive treatments.

The advent of AI is slowly revolutionising this area, offering DL-based systems able to produce ED maps on a voxel-by-voxel basis, ensuring shorter execution times and equivalent or higher accuracy in the sCT image generation with respect to atlas-based or bulk strategies [35]. The time required to produce a volumetric sCT image is a key-parameter in the evaluation of a sCT generation algorithm, especially in the context of

MRgRT. Times exceeding the order of a few minutes are not compatible with the online adaptive workflow, limiting the application only to offline procedures.

Several experiences based on DL strategies demonstrated the feasibility of providing volumetric sCT images in less than 30 seconds if the algorithms are integrated on Central Processing Unit (CPU) architectures (i.e. 21 sec in [34] and 15 sec in [35]) and in less than 10 seconds if Graphical Processing Unit (GPU)-based networks are considered (i.e. 5.6 sec in [34] and 5.7 sec in [46]).

Beyond the generation time, the quality of a sCT image is generally evaluated in terms of image and dose accuracy. The image accuracy is generally quantified by the mean error (ME) and the mean absolute error (MAE), where the first one represents the mean difference between the HU values reported in the sCT image and the corresponding ones in the CT, while the second considers for each voxel the difference in absolute value. ME is considered as an indicator of systematic offset errors in the sCT generation, while the MAE is considered as a metric of accuracy [40].

In addition to these parameters, the quality of a sCT can be evaluated by considering the dose accuracy, since the main purpose of generating these synthetic images is to be used as a basis of dose calculation of MR-based RT treatment plans. Dose accuracy is usually estimated considering the differences between the dose distribution calculated on sCT and the corresponding one obtained on the original CT. Such comparison is mainly quantified in terms of gamma analysis, generally considering 2%/2mm or 3%/3mm as tolerance criteria [40,43]. Beyond the gamma comparison, dose accuracy is also quantified in terms of Dose Volume Histogram (DVH) analysis, evaluating the variation in the estimation of DVH parameters when the treatment plan is calculated considering the ED map obtained from sCT rather than CT. The most observed parameters are generally the minimum, mean and maximum dose to some reference structures, such as PTV or OARs in proximity to the target [29,36,44].

Table 1 reports the main studies on AI for generation of synthetic CTs based on a review of the literature performed in December 2020 on Scopus, following the keywords and inclusion criteria detailed in the supplementary materials. All studies were described in terms of DL-algorithm used, anatomical region analysed, magnetic field to which MR images were acquired, image and dose accuracy of the sCT images obtained, and time to generate the sCT.

					Number Pts		Image accuracy		Gamma Analysis			
Ref	**DL**	**Magnetic Field**	**MR sequence**	**Anatomic Site**	**Train**	**Test**	**MAE (SD)**	**ME (SD)**	**3%/ 3mm**	**2%/ 2mm**	**1%/ 1mm**	**Time to sCT generation (sec)**
[46]	GAN	1.0 T	T1C	Brain	15	IV	89.3 (10.3)	NA	NA	NA	NA	5.7
	CNN			Brain	15	IV	102.4 (11)	NA	NA	NA	NA	NA
[47]	U-Net	3T	T1	Brain	47	13	81.0 (14.6)	NA	NA	NA	NA	NA
[48]	GAN	1 .5 T	T1	Brain	63	14	47.2 (11)	NA	NA	99.2 (0.8)	94.6 (2.9)	NA
[49]	2D CNN	1 .5T	T1	Brain	18	IV	84.8 (17.3)	-3.1 (21.6)	NA	NA	NA	9
[50]	dense cycleGAN	NA	T1	Brain	24	IV	55.7	NA	NA	NA	NA	>60
	U-Net	1 .5 T	T2	Brain	28	6	65.4 (4.1)	NA	NA	NA	NA	NA
	cycleGAN	1 .5 T	T2	Brain	28	6	93.9 (5.9)	NA	NA	NA	NA	NA
[34]	cGAN	1.5 T	T1	Brain	40	20	61 (14)	NA	99.9 (0.1)	99.5 (0.8)	NA	10-20
[51]	DSPC	0.35T	TRUFI	Breast	48	4	NA	17.7 (4.3)	NA	98	NA	NA
[35]	GAN	1 .5 T	T2	H&N	NA	8	82.8 (48.6)	-3.9 (12.8)	NA	NA	NA	35
[52]	CNN	3 T	T2	H&N	22	12	75 (9)	9 (11)	98.7 (1.4)	95.6 (2.9)		240
[53]	cGAN	3T	mDixon	H&N	12	11	66.9 (7.3)	15.7 (12.7)	NA	NA	NA	45
	cycleGAN	3T	mDixon	H&N	12	11	82.3 (6.4)	27.5 (15.1)	NA	NA	NA	<90
[54]	cGAN	3T	T1; T2; T1C+ T1Dixon	H&N	30	15	75.2 (11.5)	1.3 (14.8)		99.0	NA	NA
[55]	MCMP-GAN	1.5 T	T1;T2	H&N	32	IV	75.7 (14.6)	NA	NA	NA	NA	<10
[56]	U-Net	1.5 T	T2	H&N	22	10	131 (24)	-6(13)	NA	NA	NA	7
[57]	U-Net	1.5 T	T1;T2	Abdomen	54	12	57 (12)	-5(12)	NA	99.7 (0.5)	NA	NA
[58]	cGAN	0.35T	TRUFI	Abdomen	12	IV	89.8 (18.7)	NA	99 (0.8)	98.7 (1.5)	NA	NA
	cycleGAN	0.35T	TRUFI	Abdomen	12	IV	94.1 (30)	NA	99 (0.7)	98.5 (1.6)	NA	NA
[59]	U-NET	3T	T1-Dixon	Abdomen	15	31	NA	NA	NA	NA	NA	NA
[60]	RU-ACGAN	NA	mDixon	Abdomen	10	IV	NA	NA	NA	NA	NA	NA
[61]	BPGAN	NA	T1	Abdomen	10	NA	5.1 (0.5)	NA	NA	NA	NA	NA
[62]	cGAN	1.5T; 3T	T1	Abdomen	21	IV	72.9 (18.2)	NA	NA	NA	>99	NA
[36]	cGAN	0.35T	TRUFI	Abdomen	80	20	78.7 (18.5)	10.83 (12.9)	99.8 (0.2)	98.7 (1.1)	90.8 (4.5)	110 (40)
		0.35T	TRUFI	Pelvis	80	20	54.3(11.9)	1.3 (8.6)	99.2 (0.2)	99 (0.7)	89.3 (4.8)	175 (43)
[63]	CNN	3T	T2	Pelvis	39	IV	NA	NA	99.2 (0.5)	98.5 (0.7)	94.6 (5.6)	NA
[64]	eCNN	3T	T2	Pelvis	15	12	30 (10.4)	2.8 (10.3)	NA	NA	NA	NA
[65]	CNN	3T	T1	Pelvis	10	16	29.8 (7.6)	NA	NA	NA	NA	NA
[34]	cGAN	3T	Dixon	Pelvis	32	30	61 (9)	2 (8)	97	91	NA	5.6
[66]	U-Net	1 .5T	T2	Prostate	36	15	29.9 (4.8)	6.7 (5.4)	99.8	99.4	98.0	3.8–7.6
[67]	2D CNN	1.5 T	T1	Prostate	20	IV	40.5 (5.4)	NA	NA	NA	NA	5.5
	3D CNN	1.5 T	T1	Prostate	20	IV	37.6 (5.1)	NA	NA	NA	NA	5.5
[35]	U-Net L2	3T	T2	Prostate	25	14	34.4 (7.7)	-1(14.2)	NA	NA	99.2 (1)	15
	U-Net PL						36.8 (6)	3.3 (13.6)	NA	NA	99.3 (0.8)	15
	GAN L2						34.1 (7.5)	-1.1 (13.7)	NA	NA	99.1 (1)	15
	GAN PL						34.9 (6.4)	4.1 (13.9)	NA	NA	99.3 (0.9)	15
	GAN MPL						35.6 (6.2)	1.9 (13.3)	NA	NA	99.2 (0.8)	15
	GAN WMPL						35.1 (6.8)	1.2 (14.0)	NA	NA	99.3 (0.8)	15
[50]	dense cGAN	NA	T2	Prostate	20	IV	50.8	NA	NA	NA	NA	>60
[68]	cGAN	1.5T	T2	Rectum	46	44	35.1 (27.2;40.3)	0.4 (-7;-12.4)	100 (0.1)	99.8 (0.2)	99.5 (0.2)	NA

Table 1 - Main experiences emerged from the literature analysis on synthetic CT generation considering the different DL architectures, the anatomical site, the MR sequence used, the magnetic field strength and the main image and dosimetric indicators. Abbreviations: GAN: Generative Adversarial Network, T1C:T1 contrast; MAE: Mean Absolute Error, ME: Mean Error; cGAN: conditional GAN; IV: internal validation; NA: not Available

The main DL architectures used for sCT generation are the U-Net and the Generative Adversarial Networks (GAN).

U-Net consists of a series of convolutions followed by a series of deconvolutions, with skip-connections between the opposing convolution and deconvolution layers [69–71]

GAN is an emerging technique for both (semi-)supervised and unsupervised learning and consists of two competitive networks termed the generator and discriminator. In these architectures, the training is carried out by deriving backpropagation through a competitive pair network process: the generator produces images that are evaluated by the discriminator in comparison to real images. The optimisation is concluded when the discriminator is no longer able to classify the results of the generator as real or fake [72].

The feasibility of generating sCT images using DL approaches was firstly demonstrated in the brain region by Han et al, who proposed a 2D deep CNN able to obtain sCT images from 1.5 T T1-weighted MRI. Modifying the U-Net architecture proposed by Ronneberger et al some years before, the authors obtained a neural network able to generate sCT images in 9 sec, reaching accuracy levels comparable to those achievable using atlas-based methods [49,73].

Han's work was the precursor of several studies that followed in successive years, with the aim of extending this approach to other anatomical sites, while also considering MR images acquired at different magnetic field strengths or characterised by different image acquisition parameters [49]. With regard to the brain, different experiences were reported in the following years, all focused on 1.5T MRI, with the most promising results in terms of image accuracy obtained on 1.5 T T1-w MR images using a GAN architecture [48,74]. Kazemifar et al reported a MAE of 47.2±11 HU on adult patients, while Maspero et al reported 61±14 HU on paediatric cases. The 2%/2mm gamma passing rates were higher than 99% in both cases [48,75].

The most investigated site is the pelvis, with most studies published for different MR sequences and field strengths, mainly considering variants of CNN and GAN architectures. It is also in this site where the best results in terms of image and dose accuracy are reported, promoting a rapid implementation in clinical practice as demonstrated by some early experiences [76,77].

To the contrary, abdomen seems to represent one of the most challenging regions for sCT generation, likely due to the unpredictable presence of air bubbles in the hollow organs that can vary during the course of MRgRT treatment, leading to significant variation in the ED map and related dose distribution [32,33].

Only three experiences report a dose accuracy analysis on the sCT images generated in the abdomen: considering a 2%/2mm gamma passing rate, Florkow et al reported values higher than 99% using a U-Net on 1.5 T MR images, while Fu et al and Cusumano et al reported results between 98% and 99% using GAN architectures on 0.35 T MRI [36,58,78]. Such results are of great importance in the context of MRgRT, as they pave the way towards online adaptive procedures using sCT images as ED maps.

Some early experiences demonstrate the feasibility of sCT generation in head and neck and breast sites, although further studies including larger cohorts of patients are recommended before implementing MR-only radiotherapy workflows at a clinical level in these anatomical sites [51,52,79].

To the authors knowledge, no experiences using AI are reported in literature regarding the lung region, likely due to the large heterogeneity of thoracic tissues which makes the sCT generation more challenging. In conclusion, sCT generation using an AI approach is expected to play an important role in MRgRT in the next years, both to reduce geometric uncertainties and to make the clinical workflow more efficient. Especially in the pelvic and abdominal regions, where several experiences have already demonstrated clinical feasibility, gradual clinical introduction is expected to rapidly occur.

4. Automatic segmentation

The possibility to develop AI-based systems able to ensure the automatic and reliable full delineation of the therapy volumes in RT has been explored for several years, reaching remarkable results especially for CT and MR imaging modalities [80–82]. In case of MRgRT applications, in addition to the anatomical accuracy, such systems should also be fast, preferably generating a contour set in the order of a few minutes to make the online adaptive procedure tolerable for the patient [26].

Contour propagation through deformable image registration (DIR) and multi atlas-based systems were used during the past two decades to offer automatic segmentation (AS), producing results which can still be optimised in terms of time and quality of contours [83,84].

Recent studies have shown the feasibility of ML or DL approaches for AS, reporting faster results and greater generalizability to image data of new patients when compared to previous AS techniques [85,86]. Contouring results achieved to date can be directly ready for clinical use or may require some manual revisions, but in either scenario ensure significant time savings when compared to the time needed to

perform the entire procedure from scratch [87,88]. As such, AI approaches may successfully support clinicians during the online adaptive procedure.

The performance of AS systems are generally evaluated on the basis of similarity metrics that describe the degree of agreement between the contours generated by the automatic system and those manually segmented by one or more experts in the field, which are considered as ground truth [89].

Yeghiazaryan et al. classified these similarity metrics in three main categories, depending on if the comparison is carried out in terms of the size of contours (size based methods), on the degree of overlap (overlap based methods) or on the distance between the contours (surface distance based methods) [90].

A detailed mathematical representation of the most commonly used similarity metrics classified per category is reported in Table 3 of Supplementary Materials.

AS methods on MR images struggle with different challenges, typically related to the investigated anatomic site. Table 2 summarises the main characteristics and findings of AI-based experiences in automatically generating contours of therapeutic volumes from MR images as reported in literature.

As reported in Table 2, the main type of DL network used for AS is currently the Convolutional Neural Network (CNN), in both 2D or 3D modality. CNNs are widely used not only for AS, but also for sCT generation and image processing in general, after its success in the ImageNet large scale visual recognition challenge, a competition for object detection and classification run annually from 2010 [71,91–94]. The CNN is a DL network that aims to imitate the process of the human brain visual cortex, by using a number of trainable parameters that is smaller compared to other DL architectures [91].

The network optimisation is carried out using a cost function and an optimiser: the different network weights are tuned by the optimiser with the aim of minimising the cost function, using ad-hoc strategies to avoid optimisation problems [71]. Common CNN-based architectures typically used for segmentation tasks are encoder-decoder networks such as the popular U-Net, which has shown to be powerful in both AS and sCT generation. In the following paragraphs, the main concerns and challenges encountered in DL-based AS are reported per site.

Ref.	Site	B(T)	MR-Linac	MR Sequence	AI technique	Training	Pts # (train/validation/test)	Eval. Metrics	Manual ground truth with IOV	VOI	Key findings
[95]	Prostate	1.5 T	N	T2	DL + Atlas+ DIR	Unsupervised pre-training and Supervised fine tuning	NS/NS/66	DC, HD, MSD	No	Target	A mixed approach based on DL, Atlas and DIR ensures good results but at the cost of large computational times (45 min)
[96]	Prostate	NS	NS	NS	FCN	Semi-supervised learning	30/NS/10	DC	No	Target	Labeled data can effectively be integrated by unlabeled ones for training the network, thus reducing the amount of necessary data.
[97]	Prostate	1.5 T	N	T2	DeepLabV3+, U-Net	Transfer learning for DeepLabV3+ Training from scratch for U-Net	40/10/NS	DC, SDC	No	Target	Pretraining on large datasets can be effective in reducing the necessary amount of data required for training
[98]	Prostate	1.5 T	Y	T2	3D U-Net and DL to generate DVF	LF based on DVF, overlapping segments, or both	5/NS/NS	DC, 95%HD, CRE	No	Target	A mixed approach based on DL and DIR ensures faster and better results than an Atlas-based method
[99]	Prostate	3 T	N	T1 (Dixon)	CNN (DeepMedic)	LF based on DC	97/NS/53	DC, 95%HD, MSD	No	OARs	DeepMedic performs better than 3D U-net and an Atlas-based approach
[100]	Prostate	1.5 T	N	T1 (mDixon)/ T2	Machine Learning	NS	65/NS/NS	DC, 95%HD, CRE, AVD	Yes	Target & OARs	Validation of a commercial AS based on ML: AS consistent with manual ground truth
[88]	Rectum	3 T	N	T2	2D U-Net	LF based on DC	93/NS/NS	DC, HD, MDA, JC	Yes	Target	AS was consistent with ground truth including 2-observers variability
[101]	Pancreas	1.5 T	N	3D T1 / 2D T2	Sparse Dictionary Learning	K-means singular value decomposition	12/NS/NS	DC, HD, CRE	No	Target	Dictionary Learning was more accurate and computationally faster than traditional AS algorithms. It requires initial human supervision at image acquisition.
[102]	Pancreas	3 T	N	T1-DCE	CNN	LF based on cross entropy	27/ NS/13	DC, HD, MSD	Yes	Target	AS of pancreas head GTV was fast (~10 seconds) and accurate
[103]	Pancreas	0.35 T	Y	TRUFI	SVM	Active learning	NS/NS/4	DC, HD	No	OARs	First example of fast enough full AS (~ 2 minutes) for online adaptive MRgRT.
[104]	Abdomen	0.35 T	Y	TRUFI	CNN + two correction CNNs	Piecewise training	100/10/10	DC, HD	No	OARs	The use of correction CNN ensures high results for AS of all the abdominal organs
[105]	Abdomen	3 T	N	T1/Dixon	2D CNN (Dense U-Net)	Deeply supervised and multiview learning	66//16/20	DC, 95%HD, JC, MSD	No	OARs	Accurate AS in abdomen can be performed by a 2D network, faster and simpler than a 3D net, if multislice input is performed.
[106]	H&N	1.5 T	Y	DWI	CNN (3D U-Net like)	LF based on DC, and dropout of 20%	48/NS/51	DC, DADC	Yes (on a subset)	Target	Accurate and fast AS of lymph nodes on DW-MR images acquired using diagnostic MR scanner and MR-Linac both.
[107]	H&N	3 T	N	T1 / T2	3D CNN (VoxResNet)	Trained from scratch on 4-channels input patches	715/103/203	DC, MSD	Yes	Target	VoxResNet guarantees AS results comparable with manual contours from multiple human experts.

Table 1- Summary of the main properties and key-findings from the studies on AS obtained from the literature research. Abbreviations: IOV (Inter-Observer Variability), DIR (Deformable image registration) DL (Deep Learning), LF (Loss Function), ML (Machine Learning), NS (Not Specified), NA (Not Applicable), DVF (Deformable Vector Field), FCN (Fully Convolutional Network), CNN (Convolutional Neural Network), DC (Dice Coefficient or ratio), SDC (Surface Dice Coefficient or ratio), HD (Hausdorff distance (maximum)), x%HD (Hausdorff distance (x-th percentile)), MSD (Mean Surface Distance), CRE (Centroid Registration Error), AVD (Average Volume Difference), MDA (Mean Distance to Agreement), JC (Jaccard Coefficient), DADC (variation of Apparent Diffusion Coefficient)

4.1 Pelvis

The main concern of AS in prostate is the inhomogeneity in image intensity around the gland boundary and the inter-patient shape variations.

As a transition towards DL-based AS, Guo Y *et al* first extracted a feature hierarchy from prostate MR images by DL [95]. These features were used for atlas selection and a DIR model is sequentially used to refine prostate segmentation. The evaluation based on similarity metrics was satisfactory, whereas the long computing time (45 min) limited the method to off-line implementations only. One of the factors that limited the initial diffusion of DL-based AS methods was the need for large amounts of expert-labelled data to train the neural networks. To overcome this issue and obtain high quality contours with a limited amount of data, strategies such as "semi-supervised" or "transfer learning" have been critical, leading to improved results with respect to standard supervised training from scratch [96,97].

Another strategy for automatic delineation during adaptive MRgRT is using a DL network to automatically analyse the contour set created on the simulation MRI and generate a deformation vector field (DVF), which can be used to adapt the simulation contours to the anatomy of the day.

To test if a DL-based estimation of a DVF is faster than using traditional DIR methods, Eppenhof *et al* trained a 3D U-Net through a loss function which can alternatively be focused on the DVF, or on the segmentation overlap, or a combination of both. They observed that the AI approach ensured better results than a reference DIR method (Elastix, https://elastix.lumc.nl/), together with a time reduction factor of about 10^{-2} [98]. Recently, strategies to perform full AS of pelvic OARs have also been proposed; a necessary task to speed up the on-line adaptive process. In this context, Savenije et al compared the use of two DL networks (DeepMedic and 3D U-Net) with a commercial atlas based solution, observing better results with the DL strategies in terms of delineation accuracy and execution time [99].

Beyond DL approaches, AS in the pelvic district can also be obtained using ML methods, as reported by Kuisma *et al*, who clinically validated a commercial solution (Philips RTdrive Core 2.0, Philips Medical Systems, Netherlands) comparing the results provided by the AS system to those obtained using manual segmentation, including an inter-observer variability analysis [100].

4.2 Abdomen

The main challenges for multi-organ AS of abdominal MRI are represented by the huge variability in terms of shape and volume of the digestive organs (i.e. stomach, duodenum, bowel loops), together with the difficulty of having MR images without motion artefacts.

In case of pancreatic lesions, Gou *et al* compared three model-free methods with an ML approach (Sparse Dictionary Learning, SDL), including the impact of two different input scans (3D T1-w and 2D T2-w MRI). For both MR sequences, SDL was found to be the most accurate and fastest algorithm [101].

Next, Liang Y *et al* trained a CNN on 56 DCE-MR images for AS of pancreatic head tumours. At evaluation, AS differences with the ground truth were within inter-observer variability, with the advantage of requiring only 10 seconds for a full procedure if processed on a current GPU, paving the way towards online adaptive MRgRT clinical applications [102].

As regards segmentation of MR images acquired using low field MR-Linac, Liang et al proposed a support vector machine (SVM) approach mixed with a feature-based registration able to obtain high quality contours of liver, kidneys and spinal cord in 2 minutes, a time sufficient for online adaptive procedures [103].

Using a DL architecture consisting of a CNN supported by a correction network able to provide additional information about the shape and position of organs, Fu *et al* reported satisfactory results not only for liver and kidneys, but also for stomach, bowel, and even for the duodenum (further affected by inter-observer variability in recognition of its boundaries) [87]. AS per patient was fast (5 sec) and even with manual corrections, the network reduced contouring time to 25% with respect to the time required to perform the whole procedure manually from scratch. Nevertheless, AI approaches for full 3D multi-organ AS, although capturing the essential volumetric information about the shape and relative position of the abdominal organs, are still often too computationally- and time-expensive. As a fast alternative, Chen *et al* developed a new DL technique called ALAMO (Automated deep Learning-based Abdominal Multi-Organ segmentation), which combines a U-net architecture with a multi-channel additional 2D network to capture the 3D information [105]. Using the ALAMO technique on T1-w 3T MR images of 20 test patients, the authors reported high values of segmentation accuracy for most of the organs delineated (DICE ranging from 0.87 to 0.96 for nine abdominal organs, 0.8 for the duodenum), while ensuring processing times of about 18 sec, perfectly compatible with online procedures.

4.3 Head and Neck

As regards the head and neck region, Gurney-Champion et al trained a 3D U-net on DW 1.5 T MR images from 51 head and neck patients to automatically delineate lymph-node chains. Fast (55 ms) and accurate (within inter-observer variability) results were observed considering DW-images acquired using a diagnostic scanner and an MR-Linac [106].

With the aim of testing the ability of DL methods in AS of GTV for the complex case of nasopharyngeal carcinoma, Lin L et al trained a 3D U-Net and a 3D CNN with 4-channel input (VoxResNet-like) on a cohort of 813 patients [107]. The test phase was carried out on 203 patients and showed that the VoxResNet-like network outperformed U-net, ensuring no need for expert manual re-editing in almost 90% of cases.

AS was fast (about 40 sec) and able to reduce the time of human editing workload to 40%. Considering the manual contours from 2 (+1) experts as ground truth, 8 additional experts were compared to the AS. Equivalent values resulted for the similarity metrics, but with smaller interquartile variations from AS, illustrating the usefulness of AS in reducing inter-observer variability.

5. **Quantitative imaging and outcome prediction**

Under the title "*predictive models applied to imaging acquired before and during radiotherapy*" many different areas can be classified. A large part belongs to the domain of treatment response prediction based on image-based biomarkers and/or anatomical changes induced by radiation, to identify early-on those patients who will benefit from adaptive procedures, as already demonstrated in some treatment sites (i.e. rectal cancer, H&N) [11,23,108,109]. The extension of these concepts evolved towards the potential modifications of the treatment on the basis of the results of predictive models to limit toxicities and/or to safely increase the tumour dose [14,110]. The use of MRI-derived parameters for outcome prediction precedes the advent of MRgRT systems and is not limited to these: due to its better soft-tissue contrast over traditional CT based imaging and the availability of multi-parameters image sequences, MRI has emerged as one of the most promising imaging modalities in this field [17,111].

Several MRI-based predictive models have been developed in these years, not directly involving the MRgRT technologies but potentially applicable to these systems: the quantitative analysis of clinical imaging has exponentially grown with the advent of Radiomics, an image analysis strategy consisting in defining a region

of interest (ROI) on clinical images, extracting from that region a series of numerical parameters (called *features*) and possibly combining them with other clinical or genomic information to generate predictive models [112]. ROI delineation, feature extraction and model elaboration are the three main processes characterising the radiomic workflow. In early experiences, the ROIs were manually delineated by clinical specialists, radiomic features were extracted applying mathematical procedures and the models were elaborated using classical statistical methods (i.e. logistic regression)[113].

Modern AI has brought important innovations to Radiomics, offering the possibility of automating the ROI delineation process, introducing neural networks able to directly infer image features from the ROI and proposing advanced ML and DL algorithms for the predictive model elaboration [114].

Despite the recent introduction of MRgRT technology in clinical practice, the number of radiomics models obtained using MR images acquired with these systems is growing in recent years, also because the large amount of images available from a single patient, which makes this technology particularly suitable for delta Radiomics [115]. Compared to Radiomics, which analyses clinical images acquired at a single time point, delta Radiomics studies the temporal variation of radiomic features extracted from a series of images acquired over the course of treatment. The technique follows the idea that the variation of a radiomic feature over the course of therapy contains indications on the patient sensitivity and response to the on-going therapy, significantly improving the accuracy of the prediction [116,117]. Several experiences have highlighted the potential of delta radiomics, not only in MR but also in other imaging modalities. However, due to the larger amount of data needed to generate evidence compared with radiomics, multi-institutional experiences including large cohorts of patients are limited [118–120]. It is worth mentioning that increasing attention is given to the robustness of AI-based predictive models due to repeated issues of repeatability/reproducibility of the models among different institutions, which is particularly difficult for MRI due to the difficulty of image standardization. [5,121].

The main experiences reporting predictive models generated using on-board MRI are discussed in the following paragraphs, separately for high and low field systems. It should be noted that, due to the still relatively recent introduction of MRgRT technologies in the clinic, most of these experiences are based on a limited number of patients and with only short-term follow-up.

As a matter of fact, we may expect a rapid improvement in the reliability and usability of predictive models based on MRgRT-images due to the rapid increase of available patient data (possibly within multi-centric consortia). At the same time, methodologies are further refined, putting robustness and generalizability of the models as a first priority. For the same purpose, procedures of signal normalisation and image pre-processing are also expected to become increasingly important in the radiomic workflow, to compensate for the known variability between different MR diagnostic scanners and even more between on-board MR scanners implemented into different MRgRT systems [122,123].

5.1 Experiences on high field systems

The first experiences on high field hybrid systems were focused on phantom studies, with the aim of characterising the image quality offered by a 1.5T on-board MR scanner of a MRgRT system for radiomic purposes. Wang et al observed on a phantom analysis that the interference of MV X-Rays on MR imaging was minimal and that the image quality offered by the MRgRT scanner was comparable to those obtained using a diagnostic scanner with the same magnetic field strength [124].

Kooreman et al have assessed the feasibility of performing quantitative imaging on a 1.5T MR-Linac system, acquiring T1-w, T2-w, DW and DCE imaging of a phantom on four different hybrid systems, observing values in terms of accuracy, reproducibility and repeatability of the MR sequences that makes feasible and reliable quantitative imaging approaches on high field MRgRT systems [125]. To the best of our knowledge, the only clinical experience reporting quantitative imaging analysis on high field MRgRT systems is those reported by Lorentz et al, who observed on four prostate cases a significant variation in delta-radiomic profiles of bladder and rectal wall adjacent to the prostate, considering serial T2-weighted MR images acquired during MRgRT treatment [126]. However, thanks to recent findings [124,125], it should be in principle possible to apply on any high field MRgRT systems models elaborated on MR images acquired using a 1.5 T diagnostic scanner, once the compatibility in terms of MR sequence parameters is verified. A complete list of the predictive models elaborated on 1.5 T diagnostic MR scanners is reported in Table 4 of Supplementary Materials. Considering the known variability of MRI-based models for acquisition parameters, it is strongly advised to perform an external validation study on a cohort of patient data acquired using MRgRT technology before applying a predictive model in clinical practice [59,70].

5.2 Experiences on low field systems

During the early period of MRgRT implementation, the question was raised whether the image quality offered by on-board low field MR scanners was sufficient to perform quantitative analysis, especially considering that these systems exhibited characteristics not usual in terms of image sequence and magnetic field strength. Different hypothesis-generating studies were conducted on low field MR images, with the aim of demonstrating the feasibility of extracting image-based biomarkers. These experiences reported promising preliminary results in predicting treatment response, supporting the need to set-up more advanced studies including larger cohorts of patients [117,128,129].The first preliminary experience was reported by Boldrini et al, who identified two delta radiomics features on low field MR images of 16 patients affected by locally advanced rectal cancer (LARC) able to predict clinical complete response after MRgRT [117]. These features, measuring the variation of two parameters (least length according to principal component analysis and grey level non uniformity based on run length matrix) after two weeks of treatments, reported higher discriminative performance with respect to radiomics features calculated at a single time-point, results are partially confirmed in successive validation studies [130]. However, no predictive model was proposed due to the small number of patients.

Two experiences were reported in pancreatic cancer, which is one of the most interesting regions considering the benefits and the potentialities of the online adaptive MRgRT procedures [11].

Simpson et al first proposed two predictive models based on Random Forest and LASSO regression, both able to predict the treatment outcome in 20 patients affected by unresectable pancreatic cancer with an AUC of 0.81. The models analysed the variation of radiomic features on all five MRgRT treatment fractions, identifying as most predictive parameters two textural features based on co-occurrence and size zone matrices [128]. On the same anatomical region, Cusumano et al identified a delta radiomics feature, the variation of the cluster shade calculated on the co-occurrence matrix when a biologically effective dose value of 40 Gy was reached, able to predict local control one year after the end of treatment with an AUC of 0.78. The study was conducted on 35 patients belonging to two institutions and used a linear logistic regression for model elaboration [116]. Other experiences on low field MRgRT systems were focused on the analysis of Apparent diffusion coefficient (ADC) maps. In a first experience using an MRI-Cobalt system, Yang et al reported the feasibility of DWI acquisition on a 0.35 T MRgRT system, measuring an ADC value in

agreement with the reference within 5% of error in longitudinal direction [129]. From this observation, the same authors observed that a delta radiomics analysis of ADC maps is able to predict the treatment effective score (TES) of patients affected by soft tissue sarcoma. Including delta radiomic features extracted from longitudinal DW MR images in an SVM, the authors were able to predict the TES on 30 patients, reporting an AUC value of 0.91±0.05 [131].

Beyond these experiences focused on radiomic analysis, a series of predictive models based on the evaluation of simple morphological indicators are being introduced into the MRgRT community, with the advantage of being simpler to calculate and more prone to be immediately useable: as mentioned before, the use of ML and DL algorithms in predictive modelling is indeed a debated topic in the scientific community, as these algorithms act as black-box systems, limiting their clinical interpretability of the models, and then their clinical diffusion. A relevant example in this context is represented by the Early Regression Index (ERI), a morphological parameter that aims to model tumour regression during the first weeks of neoadjuvant radio-chemotherapy by means of a function of the tumour volume measured on MR images acquired at simulation and at mid-therapy, on the basis of radiobiological considerations [108]. An example of volumetric regression in case of rectal cancer using MRgRT technology is reported in Figure 4.

In a first experience on rectal cancer, Fiorino et al demonstrated that this simple parameter, if calculated on MR images acquired with a 1.5 T diagnostic scanner, was able to identify patients who would have pathological complete response during RT treatment, with an AUC of 0.81 calculated on 64 patients, with extension and confirmation of these findings on a larger population [108,132]. The same parameter was also tested in an external validation study carried out on 52 patients treated with two 0.35T MRgRT systems, reporting high discriminative performance (AUC=0.93) also on low field MRgRT systems [133].

Although first applied to model rectal cancer regression, a recent preliminary experience has also evaluated the feasibility of using this index for outcome prediction of patients affected by cervical cancer, reporting an AUC of 0.84 on 16 patients [134].

In conclusion, the use of predictive models in MRgRT is expected to grow in the next few years, making optimal use of the information that can be extracted from the daily MR acquisitions. Considering that technological development is leading to a strong acceleration of the online adaptive procedure, it is reasonable to expect that in the near future the acquisition of images in parallel with the adaptive procedure

will be possible, opening the possibility of developing predictive models on MRI sequences different from those used for patient positioning, further improving their predictive capabilities.

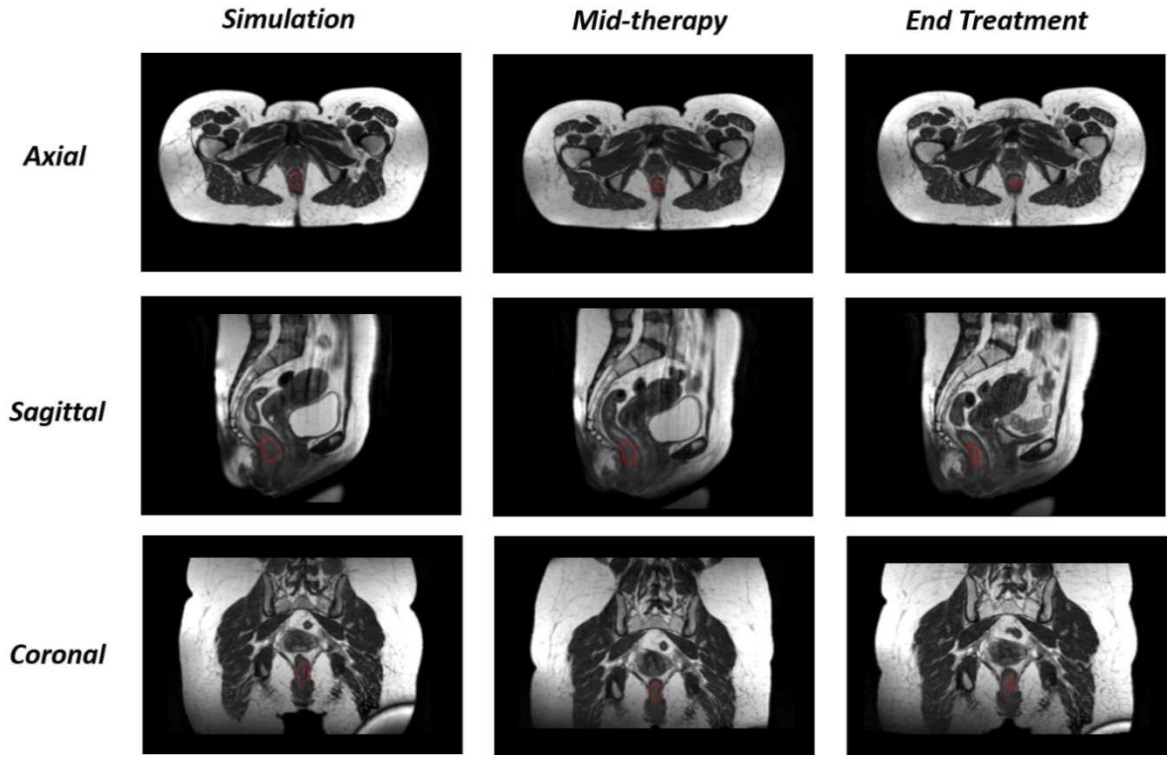

Figure 4 - Example of rectal cancer regression observed using an MRgRT technology on axial (top), sagittal (middle) and coronal (bottom) acquired during simulation, mid therapy and end treatment

6. **Advanced imaging and motion management**

An on-board MR scanner, with its ability to provide high soft tissue contrast without ionising radiation, offers great potential to efficiently manage intra-fraction motion without external surrogates and efficiently monitor short and long-term breathing variations [135,136].

To date, the clinical on-board high temporal resolution dynamic MR acquisition during treatment delivery is only available in 2D modality; therefore, the current MRgRT systems do not provide detailed information on the 3D target motion trajectory or out-of-plane OARs motion [16,137]. AI strategies have recently been proposed to infer the 3D motion trajectory from multi-slice 2D images or even reconstruct 3D acquisitions, opening the way towards real-time volumetric motion management strategies [138].

The first AI-based experiences on online MR imaging were focused on the elaboration of tracking algorithms designed for 2D MR images, with the aim of auto-segmenting the lesion in real-time and estimating its 2D position. In 2011, Cervino et al proposed two tracking algorithms for tumour motion estimation from 2D

cine MRI of the lungs. The first consisted of a template matching (TM) technique in combination with a diaphragm-based surrogate signal, while the second was an ANN based on principal component analysis (PCA) [139]. In a cohort of 5 patients imaged using a 3T MR scanner, the authors observed that the TM technique performed better than the ANN and that out-of-plane motion could also be tracked using the diaphragm as a motion surrogate. Subsequently, a pulse-coupled neural network (PCNN) was proposed for lung AS on low field MR images (0.5 T), reporting 87-92% of agreement with respect to manual contouring and a centroid tracking accuracy within 1.5 mm [140].

Fast et al then applied the PCNN architecture proposed in [141] on 1.5 T MR images, comparing the results with those achieved using a conventional algorithm based on multi-template (MT) and intensity-based DIR. In the study the authors observed that MT-DIR algorithms performed slightly better than PCNN, but the neural network training was performed on a set of only 10 images, while in [140] the PCNN was trained on 30 images [141]. Automatic real-time segmentation of lung lesions was also demonstrated with ML methods, combining a sequential Monte Carlo (MC) method based on Bayesian probability (named *particle filtering*) with an autoregressive model in a 2D motion prediction algorithm that sequentially tracks, contours and predicts the tumour position 250 ms in advance using 1.5T MR images acquired at 4 frames/second. With root mean square (RMS) tracking errors averaged over 7 patients of 1.3±0.5 mm and 2.0 ±0.8 mm with and without prediction, respectively, the authors showed the advantages of the model proposed [142].

In the following years, several ML or DL algorithms for robust estimation of 2D motion trajectories were proposed and different experiences have shown the possibility to predict 2D motion of targets different from lung cancer or to simultaneously track multiple ROIs in the same image [143]. Dhont et al also illustrated the use of a tracking-learning-detection methodology to recover from brief moments of out of slice motion of the target in 2D motion tracking [144,145].

Several DL-based methods have been proposed to speed up the image reconstruction step of the real-time MR acquisitions, as this step represents the largest component of latency in the MRgRT treatment delivery. Terpstra et al compared four combinations of conventional and DL-based methods, with the aim of obtaining an architecture for fast reconstruction of 1.5 T 2D cine MRI and to accurately estimate the motion of abdominal lesions [146]. Based on data from a cohort of 135 cases, the authors identified as best combination the use of a conventional method for image reconstruction (Non-Uniform Fast Fourier

Transform, NUFFT) and a DL architecture for motion quantification (SPyNET), obtaining an imaging frame rate of 25 Hz with a RMSE<1 mm. DL approaches have also produced interesting results in cardiac MR imaging, which represents a challenging area for MR acquisition due to the intrinsic high frequency motion of the heart [147–149]. A convolutional recurrent neural network was recently proposed on 2D cine MR acquisitions, demonstrating the possibility of reconstructing high quality cardiac MR images from highly under-sampled k-space data [148,150,151]. Ghodrati et al. explored and optimised the network structures and loss functions used in DL-based cardiac cine image reconstruction [152].

Besides 2D applications, there is a growing interest towards 3D applications as breathing-induced tumour motion often follows a three dimensional motion path due to phenomena like hysteresis, baseline drift or cardiac motion [135,136,151,153,154]. Several groups have investigated the possibility to extract 3D motion information from the real-time 2D images, registering the 2D MR images with 3D MRI volumes acquired at the same imaging condition and then generating models based on PCA analysis of the deformation vector fields obtained by the registration of 2D and 3D MR images [155–157].

However, these approaches suffered from different limitations due to the fact that the 3D MRI volumes showed image artifacts due to retrospective sorting and a comparative phantom study demonstrated to fail in predicting 3D motion when deviation from the average breathing cycle were present on 2D MR images [158]. Alternative approaches were proposed to overcome the lack of data to train 4D motion models by using surrogate signals derived from 2D MR images [159,160]. Another possibility is represented by the combination of single and multi-slice MR image information, as reported by Ginn et al who demonstrated the feasibility of obtaining out of slice tumour motion information from the analysis of 2D MR images by using ML models trained on the DVFs calculated among the 10 most recent images and a reference image [161,162]. While the model agreed well with gating directly on high frame-rate images, out-of-plane motion remains an issue and the use of an internal image-based surrogate will likely be more precise.

With regards to 3D MR acquisitions in real-time, high quality 3D MRI at acquisition speeds capable of capturing breathing-induced motion, or with a total system latency below 500 milliseconds as recommended by the AAPM Task Group report 76, is currently not available on MRgRT systems, due to spatial-temporal limitations in the image acquisition [163].These acquisitions are much more time consuming due to the need to encode a third spatial dimension, and it requires a substantial boost in achievable acceleration factors in

order to perform these acquisitions in real time. Although non-Cartesian k-space sampling methods, such as spirals, could be used to further accelerate the acquisition, the nuances of non-Cartesian image reconstruction and the numerous challenges in sampling trajectory calibration and image blurring are important issues to be addressed. Some research groups have focused on post-processing methods to increase the spatial resolution of 3D MR data that were acquired through sparse sampling at high temporal resolution in order to obtain qualitative volumetric MRI in real-time. To this end, DL-based super-resolution (SR) techniques have been particularly promising. Kim et al. proposed a combination of 3D dynamic keyhole imaging with a cascaded DL-based SR model [164]. Through this technique, high-temporal (420 ms) but low-spatial resolution ($6\times6\times6$ mm^3) 3D MRI data acquired on a clinical MRgRT system could be converted to a 4 times higher in-plane spatial resolution ($1.5\times1.5\times6$ mm^3) with only a limited increase (<100 ms) in total acquisition time [164]. A recent experience demonstrated that the reduced through-plane spatial resolution can be improved by using a super-resolution technique based on an enhanced deep residual network in a framework called SMORE (Synthetic Multi-Orientation Resolution Enhancement), that can be applied to both 3D and 2D data where it also succeeds in removing anti-aliasing artefacts [165].

7. **Automatic planning**

Treatment planning is one of the most time consuming and operator dependent steps in the RT workflow. In the last years, many advancements through AI have led to the development of different automatic treatment planning (ATP) approaches which aim to reduce human intervention and workload, ideally standardising and improving the quality of treatment plans in parallel [166,167].

In general, ATP has been an area of active research since several years with a growing body of literature. However, it has not been thoroughly investigated in the context of MRgRT. The ATP approach in MRgRT would not differ substantially from conventional RT, except from two main aspects; the need to consider the presence of the magnetic field in dose calculations and the requirement to provide fast results in terms of plan generation, to make the technique suitable for online adaptive procedures.

The feasibility of integrating an ATP strategy within an online adaptive RT workflow have already been investigated in CBCT-guided radiotherapy, with a commercial solution recently made available [168].

It is expected that online adaptation may be optimal when coupled to MRgRT due to superior soft tissue contrast and absence of imaging radiation dose. Based on the current literature, three main ATP paradigms have been proposed for clinical practice [167,169]:

- Knowledge-based planning (KBP), which uses prior knowledge and experience to predict an achievable dose in a new patient of a similar population or to derive a better starting point for further manual optimisation.
- Template-based (TB) automatic planning, which generates a treatment plan starting from a user-defined protocol with goals and objectives.
- Multi-criteria optimisation (MCO), which identifies the optimal plan on a previously created once the Pareto surface has been created starting from the definition of a wish-list containing clinical objectives

These different ATP approaches are here revisited in the MRgRT perspective, especially considering the online adaptive procedure since off-line ATP in MRgRT can be considered similar to what is done in conventional RT. TB planning is to some extent already manually implemented during the online adaptive MRgRT procedure. Since the starting point of the adapted plan is the plan optimised during simulation, clinical objectives are already defined and the plan proposed by the optimiser during the online adaptation aims to satisfy the wish-list defined during simulation. What is missing is the implementation of an AI system which simulates the reasoning behaviour of a human planner to automatically adjust the optimisation parameters during the online optimisation. The KBP approach could be interesting for the MRgRT application to obtain a fast prediction with dose constraints compliance given the daily relationship among target and OARs, as already demonstrated in different experiences [170,171].

Concerning the MCO approach, the “a posteriori” solution (which consists in the generation of a database of pareto optimal plans that can be interactively navigated by the planner to choose the clinically optimal plan) is not suitable for MRgRT, mainly due to time constraints [172]. The a priori MCO solution, which consists in generating a single pareto-optimal plan based on a site-specific protocol defined by the clinicians, can instead be an efficient solution for MRgRT online adaptive applications as it directly provides a single planning solution. Some commercial solutions based on this technique for MRgRT are expected to be available in the next years [173]. To date, the only published experience on ATP in MRgRT was performed on a high field MR-Linac. In a cohort of 23 patients affected by LARC, the use of MCO demonstrated

superior automated plans over the manual plans in terms of OARs dose sparing, reduction of MU delivered (-13% using ATP) and computation treatment time (-15% using ATP) [174]. Wang et al have recently published a review on DL applications incorporated in the main steps of ATP: beam selection, dose prediction, fluence generation and delivery parameters generation [175]. As another AI-based ATP strategy, deep reinforcement learning appears to be extremely suitable, even though some further development should be performed before considering it for clinical implementation [176]. Due to a limited number of MRgRT units in the world and the consequent reduced number of patients treated with this technology, multi-institutional studies are needed to collect large amounts of MR-based treatment plans to train MRgRT-specific ATP systems. The diffusion of automatic systems for treatment planning in MRgRT will allow more reliable adaptive procedures, allowing treatment personalisation on the basis of image-based, dose-based or genome-based biomarkers, as already demonstrated in some preliminary experiences [177–179]

8. **Automation in QA**

Medical physicists spend a substantial amount of their time in an RT department working on QA tasks, independently of the presence of MRgRT units; such tests are related to machine characterisation (commissioning, patient specific QA, periodic QA, end-to-end), to the equipment used for measurements or to the software adopted in daily clinical activity [22]. As these tests can take between 20 to 150 minutes for a single patient, there is a potential for AI tools not only to streamline the process reducing the time needed but also to standardise decisions and minimise errors. In an online adaptive MRgRT treatment, AI solutions for patient specific QA would have a high clinical impact, especially considering the fact that the QA result has to be provided in a few seconds, while the patient is waiting in treatment position [180,181]. In vivo dosimetry systems based on inorganic scintillators are under development to provide real-time dosimetric information during beam delivery, but they are still far from clinical implementation also because they are not able to provide 3D measurements at this stage of development [182,183]. The AI growth is leading the automatization of a lot of QA processes in conventional RT, and it is reasonable to assume that most of these innovations will soon be implemented in MRgRT as well, although no dedicated experiences have been published so far. McNutt et al showed that using data collected over several years on patient specific QA, it is possible to perform a more thorough evaluation of the key QA steps and to automate and personalise the

QA methods, resulting in a more efficient and safe evaluation for each individual patient [184]. A new patient treatment could be compared to the one of similar patients in their patient cohort and any dissimilarity can be detected and further investigated. Thanks to this approach, guideline adherence, patient contours, plan quality, pre-treatment verification results can be checked [184].

This comparison can be performed using simple statistical methods or more sophisticated classification models based on ML or DL, which require a large amount of data and collaborative continuous efforts to make the models portable and usable in different institutions.

With the aim of detecting potential errors in a treatment plan, Kalet et al developed a ML approach based on a Bayesian network for chart checking. The network was constructed using a RO ontology and employed an expectation maximisation algorithm to develop the conditional probability tables, using as database of the historic clinical data from their clinical oncology information management system [185].

These probabilistic descriptions allowed verification of treatment plan parameters to be within the normal scope of practice and therefore the detection of potential outliers to be flagged for further investigation.

Other groups have developed knowledge-based methods for dose and DVH predictions to be used for plan quality assessment. The plan produced for a specific patient is compared to the predicted plan obtained using the ATP system, as such allowing an easy identification of the plans that require further optimisation [186].

A similar approach was proposed by Nguyen et al, who created a CNN-based system able to predict the optimal dose distribution for each single patient in case of prostate cancer [187].

Regarding patient specific QA, two different approaches have been reported in literature to minimise or even avoid the pre-treatment measurements required for this specific task. The first approach consists in identifying the most challenging plans to be checked, while the second approach consists in predicting the gamma passing rate starting from a series of plan information data such as dose features, plan complexity, machine model, beam energy, type of multi leaf collimator (MLC) and jaw positions [188,189].

Lam et al proposed three ML algorithms able to predict the results of 2%/2mm gamma passing rates obtained with portal dosimetry for IMRT QA. The authors observed a prediction accuracy of these algorithms ranging from 95% and 98% [190]. Li et al proposed a ML architecture consisting of a Poisson Lasso (PL) regression model that predicts the individual gamma passing rate, followed by a RF classification model that classifies the QA result as “pass” or “fail”. The system was reported to have reliable results once the original data was

pre-processed to compensate for the original tendency of PL model in overestimating the gamma passing rates of challenging VMAT plans [191]. As discussed, these ML approaches also have the advantage of interpretability and they allow to discriminate the features that have the highest impact on the results. On the other side, these models have low portability as they are highly dependent on different factors that are institution-dependent, such as the systems used for pre-treatment verification, the evaluation methodology chosen and the treatment unit. DL methods have also been proposed to extract features from the dataset that can be used to model and classify pre-treatment verification results [192–195]. Lastly, it is worth mentioning that the integration of DL and radiomics could have great potential in the growth of automation in QA, as reported by a recent experience by Nyflot et al, which demonstrated that a DL model can detect the presence of treatment delivery errors from the radiomic analysis of patient-specific QA dose maps. In the future, it is reasonable to expect that thanks to the support of modern AI-based systems it will be possible to automate QA procedures in MRgRT as well, so reducing the time needed for plan specific verifications without compromising safety and quality of online adaptive procedures.

9. **Clinical considerations and final remarks**

The present work reports the state of art in AI applications for MRgRT. While in some of the evaluated fields several studies have already been published and broad clinical use is to be expected within the near future, this seems further away in other fields. However, all the fields discussed are subject to ongoing research aiming to address specific clinical needs. From a clinical point of view, AI is expected to allow faster adaptive treatments for the patients in the near future, thanks to the development of suitable online procedures characterised by treatment times comparable to those typical of conventional RT. This process is not limited to MRgRT but involves other approaches using different in-room imaging systems, such as CBCT, and commercially available solutions started to appear [168].

With regard to online adaptive treatments, the main anticipated clinical advantage that AI has to offer is the reduction of the treatment time slot. Shortening adaptive treatments will also reduce intra-fraction organ variability, thereby ensuring not only less exhausting but also safer treatments for patients, with a significant impact not only for breath hold treatments, but also for free-breathing ones [196,197].

In addition to making treatment procedures faster, it is reasonable to assume that the development of AI-based systems capable of predicting treatment outcome may support in the future more advanced concepts of adaptive radiotherapy, where not only the shape of the dose distribution is adapted to anatomical modifications, but also the whole therapeutic approach. An example of this concept is the adaptation of the dose prescription, increasing the fractional dose during RT in case of poorly responding patients, with the aim of increasing the therapeutic efficacy. An important AI contribution is also expected in dose escalation studies, where it is necessary to define new dosimetric constraints for OARs. Several dose escalations studies have already been started in MRgRT with the aim of defining new dose constraints that reflect the improvement in terms of accuracy in dose delivery obtained with these modern technologies.

The room for AI application mentioned in this review, despite the limited published experience, is huge with relevant potentials for clinically relevant improvements. On-line ATP and automated QA have the potential to better quantify the complex effects of various different influencing parameters on the applied dose to the patient, thereby potentially making it easier to establish standards and to adhere to best practices. Especially in these aspects, collaborative multi-institutional efforts on training AI-models are warranted. In general, guidelines and recommendations are also necessary for the translation of AI methods from research to a broad implementation in clinical practice. It will be the responsibility of medical physicists to analyse uncertainties, discover limitations, elaborate thresholds and action levels in order to assess their impact on patient treatments [3]. On the other side, companies and vendors of AI systems have the responsibility of providing sufficient information and more open access to the original data on which they based the development of their artificial systems [198].

Another aspect that has to be necessarily addressed for a full and safe clinical implementation of AI in MRgRT concerns ethics. A clear assignment of responsibility has to be defined in case of an error performed by an AI-based system. This represents a central issue in the whole clinical landscape and also in all the applications that are exploited in clinical medicine by AI today and likely translating into new tasks for commissioning and QA of AI-based systems for medical physicists [3,199]. In conclusion, the integration of AI will presumably improve the quality of MRgRT treatments significantly in the coming years and may also play a key role in the endeavour to individualise cancer treatments.

References

[1] LeCun Y, Bengio Y, Hinton G. Deep learning. Nature 2015;521:436–44. https://doi.org/10.1038/nature14539.

[2] Francolini G, Desideri I, Stocchi G, Salvestrini V, Ciccone LP, Garlatti P, et al. Artificial Intelligence in radiotherapy: state of the art and future directions. Med Oncol 2020;37:50. https://doi.org/10.1007/s12032-020-01374-w.

[3] Vandewinckele L, Claessens M, Dinkla A, Brouwer C, Crijns W, Verellen D, et al. Overview of artificial intelligence-based applications in radiotherapy: Recommendations for implementation and quality assurance. Radiotherapy and Oncology 2020;153:55–66. https://doi.org/10.1016/j.radonc.2020.09.008.

[4] Bibault J-E, Giraud P, Burgun A. Big Data and machine learning in radiation oncology: State of the art and future prospects. Cancer Letters 2016;382:110–7. https://doi.org/10.1016/j.canlet.2016.05.033.

[5] Kulkarni S, Seneviratne N, Baig MS, Khan AHA. Artificial Intelligence in Medicine: Where Are We Now? Academic Radiology 2020;27:62–70. https://doi.org/10.1016/j.acra.2019.10.001.

[6] Lambin P, van Stiphout RGPM, Starmans MHW, Rios-Velazquez E, Nalbantov G, Aerts HJWL, et al. Predicting outcomes in radiation oncology—multifactorial decision support systems. Nature Reviews Clinical Oncology 2013;10:27–40. https://doi.org/10.1038/nrclinonc.2012.196.

[7] Fiorino C, Jeraj R, Clark CH, Garibaldi C, Georg D, Muren L, et al. Grand challenges for medical physics in radiation oncology. Radiother Oncol 2020;153:7–14. https://doi.org/10.1016/j.radonc.2020.10.001.

[8] Thompson RF, Valdes G, Fuller CD, Carpenter CM, Morin O, Aneja S, et al. Artificial intelligence in radiation oncology: A specialty-wide disruptive transformation? Radiotherapy and Oncology 2018;129:421–6. https://doi.org/10.1016/j.radonc.2018.05.030.

[9] Jaffray DA. Image-guided radiotherapy: from current concept to future perspectives. Nat Rev Clin Oncol 2012;9:688–99. https://doi.org/10.1038/nrclinonc.2012.194.

[10] Fiorino C, Guckemberger M, Schwarz M, van der Heide UA, Heijmen B. Technology-driven research for radiotherapy innovation. Mol Oncol 2020;14:1500–13. https://doi.org/10.1002/1878-0261.12659.

[11] Boldrini L, Cusumano D, Cellini F, Azario L, Mattiucci GC, Valentini V. Online adaptive magnetic resonance guided radiotherapy for pancreatic cancer: state of the art, pearls and pitfalls. Radiat Oncol 2019;14:71. https://doi.org/10.1186/s13014-019-1275-3.

[12] Murray J, Tree AC. Prostate cancer - Advantages and disadvantages of MR-guided RT. Clin Transl Radiat Oncol 2019;18:68–73. https://doi.org/10.1016/j.ctro.2019.03.006.

[13] Chiloiro G, Boldrini L, Meldolesi E, Re A, Cellini F, Cusumano D, et al. MR-guided radiotherapy in rectal cancer: First clinical experience of an innovative technology. Clin Transl Radiat Oncol 2019;18:80–6. https://doi.org/10.1016/j.ctro.2019.04.006.

[14] Corradini S, Alongi F, Andratschke N, Belka C, Boldrini L, Cellini F, et al. MR-guidance in clinical reality: current treatment challenges and future perspectives. Radiat Oncol 2019;14:92. https://doi.org/10.1186/s13014-019-1308-y.

[15] Klüter S. Technical design and concept of a 0.35 T MR-Linac. Clinical and Translational Radiation Oncology 2019;18:98–101. https://doi.org/10.1016/j.ctro.2019.04.007.

[16] Lagendijk JJW, Raaymakers BW, van Vulpen M. The magnetic resonance imaging-linac system. Semin Radiat Oncol 2014;24:207–9. https://doi.org/10.1016/j.semradonc.2014.02.009.

[17] Pollard JM, Wen Z, Sadagopan R, Wang J, Ibbott GS. The future of image-guided radiotherapy will be MR guided. Br J Radiol 2017;90:20160667. https://doi.org/10.1259/bjr.20160667.

[18] Gurney-Champion OJ, Mahmood F, van Schie M, Julian R, George B, Philippens MEP, et al. Quantitative imaging for radiotherapy purposes. Radiotherapy and Oncology 2020;146:66–75. https://doi.org/10.1016/j.radonc.2020.01.026.

[19] Yang Y, Cao M, Sheng K, Gao Y, Chen A, Kamrava M, et al. Longitudinal diffusion MRI for treatment response assessment: Preliminary experience using an MRI-guided tri-cobalt 60 radiotherapy system. Med Phys 2016;43:1369–73. https://doi.org/10.1118/1.4942381.

[20] Mutic S, Dempsey JF. The ViewRay system: magnetic resonance-guided and controlled radiotherapy. Semin Radiat Oncol 2014;24:196–9. https://doi.org/10.1016/j.semradonc.2014.02.008.

[21] Lagendijk JJW, Raaymakers BW, van Vulpen M. The magnetic resonance imaging-linac system. Semin Radiat Oncol 2014;24:207–9. https://doi.org/10.1016/j.semradonc.2014.02.009.
[22] Kurz C, Buizza G, Landry G, Kamp F, Rabe M, Paganelli C, et al. Medical physics challenges in clinical MR-guided radiotherapy. Radiation Oncology 2020;15:93. https://doi.org/10.1186/s13014-020-01524-4.
[23] Lim-Reinders S, Keller BM, Al-Ward S, Sahgal A, Kim A. Online Adaptive Radiation Therapy. Int J Radiat Oncol Biol Phys 2017;99:994–1003. https://doi.org/10.1016/j.ijrobp.2017.04.023.
[24] Bohoudi O, Bruynzeel AME, Senan S, Cuijpers JP, Slotman BJ, Lagerwaard FJ, et al. Fast and robust online adaptive planning in stereotactic MR-guided adaptive radiation therapy (SMART) for pancreatic cancer. Radiother Oncol 2017;125:439–44. https://doi.org/10.1016/j.radonc.2017.07.028.
[25] Lamb J, Cao M, Kishan A, Agazaryan N, Thomas DH, Shaverdian N, et al. Online Adaptive Radiation Therapy: Implementation of a New Process of Care. Cureus 2017;9:e1618. https://doi.org/10.7759/cureus.1618.
[26] Güngör G, Serbez İ, Temur B, Gür G, Kayalılar N, Mustafayev TZ, et al. Time Analysis of Online Adaptive Magnetic Resonance–Guided Radiation Therapy Workflow According to Anatomical Sites. Practical Radiation Oncology 2020;0. https://doi.org/10.1016/j.prro.2020.07.003.
[27] Placidi L, Cusumano D, Boldrini L, Votta C, Pollutri V, Antonelli MV, et al. Quantitative analysis of MRI-guided radiotherapy treatment process time for tumor real-time gating efficiency. Journal of Applied Clinical Medical Physics n.d.;n/a. https://doi.org/10.1002/acm2.13030.
[28] Olberg S, Green O, Cai B, Yang D, Rodriguez V, Zhang H, et al. Optimization of treatment planning workflow and tumor coverage during daily adaptive magnetic resonance image guided radiation therapy (MR-IGRT) of pancreatic cancer. Radiat Oncol 2018;13:51. https://doi.org/10.1186/s13014-018-1000-7.
[29] Kim J, Garbarino K, Schultz L, Levin K, Movsas B, Siddiqui MS, et al. Dosimetric evaluation of synthetic CT relative to bulk density assignment-based magnetic resonance-only approaches for prostate radiotherapy. Radiat Oncol 2015;10:239. https://doi.org/10.1186/s13014-015-0549-7.
[30] Paulson ES, Ahunbay E, Chen X, Mickevicius NJ, Chen G-P, Schultz C, et al. 4D-MRI driven MR-guided online adaptive radiotherapy for abdominal stereotactic body radiation therapy on a high field MR-Linac: Implementation and initial clinical experience. Clinical and Translational Radiation Oncology 2020;23:72–9. https://doi.org/10.1016/j.ctro.2020.05.002.
[31] Mittauer KE, Hill PM, Bassetti MF, Bayouth JE. Validation of an MR-guided online adaptive radiotherapy (MRgoART) program: Deformation accuracy in a heterogeneous, deformable, anthropomorphic phantom. Radiother Oncol 2020;146:97–109. https://doi.org/10.1016/j.radonc.2020.02.012.
[32] Cusumano D, Teodoli S, Greco F, Fidanzio A, Boldrini L, Massaccesi M, et al. Experimental evaluation of the impact of low tesla transverse magnetic field on dose distribution in presence of tissue interfaces. Physica Medica 2018;53:80–5. https://doi.org/10.1016/j.ejmp.2018.08.007.
[33] Raaijmakers AJE, Raaymakers BW, Lagendijk JJW. Experimental verification of magnetic field dose effects for the MRI-accelerator. Phys Med Biol 2007;52:4283–91. https://doi.org/10.1088/0031-9155/52/14/017.
[34] Maspero M, Savenije MHF, Dinkla AM, Seevinck PR, Intven MPW, Jurgenliemk-Schulz IM, et al. Dose evaluation of fast synthetic-CT generation using a generative adversarial network for general pelvis MR-only radiotherapy. Phys Med Biol 2018;63:185001. https://doi.org/10.1088/1361-6560/aada6d.
[35] Largent A, Barateau A, Nunes J-C, Mylona E, Castelli J, Lafond C, et al. Comparison of Deep Learning-Based and Patch-Based Methods for Pseudo-CT Generation in MRI-Based Prostate Dose Planning. Int J Radiat Oncol Biol Phys 2019;105:1137–50. https://doi.org/10.1016/j.ijrobp.2019.08.049.
[36] Cusumano D, Lenkowicz J, Votta C, Boldrini L, Placidi L, Catucci F, et al. A deep learning approach to generate synthetic CT in low field MR-guided adaptive radiotherapy for abdominal and pelvic cases. Radiother Oncol 2020;153:205–12. https://doi.org/10.1016/j.radonc.2020.10.018.
[37] Mittauer KE, Hill PM, Geurts MW, De Costa A-M, Kimple RJ, Bassetti MF, et al. STAT-ART: The Promise and Practice of a Rapid Palliative Single Session of MR-Guided Online Adaptive Radiotherapy (ART). Front Oncol 2019;9. https://doi.org/10.3389/fonc.2019.01013.

[38] J J, T N, K S. The rationale for MR-only treatment planning for external radiotherapy. Clinical and Translational Radiation Oncology 2019;18. https://doi.org/10.1016/j.ctro.2019.03.005.
[39] Owrangi AM, Greer PB, Glide-Hurst CK. MRI-only treatment planning: benefits and challenges. Phys Med Biol 2018;63:05TR01. https://doi.org/10.1088/1361-6560/aaaca4.
[40] Edmund JM, Nyholm T. A review of substitute CT generation for MRI-only radiation therapy. Radiat Oncol 2017;12:28. https://doi.org/10.1186/s13014-016-0747-y.
[41] Vanquin L, Boydev C, Korhonen J, Rault E, Crop F, Lacornerie T, et al. Radiotherapy treatment planning of prostate cancer using magnetic resonance imaging. Cancer/Radiotherapie 2019;23:281–9. https://doi.org/10.1016/j.canrad.2018.09.005.
[42] Jonsson JH, Karlsson MG, Karlsson M, Nyholm T. Treatment planning using MRI data: an analysis of the dose calculation accuracy for different treatment regions. Radiat Oncol 2010;5:62. https://doi.org/10.1186/1748-717X-5-62.
[43] Johnstone E, Wyatt JJ, Henry AM, Short SC, Sebag-Montefiore D, Murray L, et al. Systematic Review of Synthetic Computed Tomography Generation Methodologies for Use in Magnetic Resonance Imaging-Only Radiation Therapy. Int J Radiat Oncol Biol Phys 2018;100:199–217. https://doi.org/10.1016/j.ijrobp.2017.08.043.
[44] Cusumano D, Placidi L, Teodoli S, Boldrini L, Greco F, Longo S, et al. On the accuracy of bulk synthetic CT for MR-guided online adaptive radiotherapy. Radiol Med 2019. https://doi.org/10.1007/s11547-019-01090-0.
[45] Prior P, Chen X, Gore E, Johnstone C, Li XA. Technical Note: Is bulk electron density assignment appropriate for MRI-only based treatment planning for lung cancer? Med Phys 2017;44:3437–43. https://doi.org/10.1002/mp.12267.
[46] Emami H, Dong M, Nejad-Davarani SP, Glide-Hurst CK. Generating synthetic CTs from magnetic resonance images using generative adversarial networks. Med Phys 2018. https://doi.org/10.1002/mp.13047.
[47] Gupta D, Kim M, Vineberg KA, Balter JM. Generation of synthetic CT images from MRI for treatment planning and patient positioning using a 3-channel U-net trained on sagittal images. Frontiers in Oncology 2019;9. https://doi.org/10.3389/fonc.2019.00964.
[48] Kazemifar S, McGuire S, Timmerman R, Wardak Z, Nguyen D, Park Y, et al. MRI-only brain radiotherapy: Assessing the dosimetric accuracy of synthetic CT images generated using a deep learning approach. Radiotherapy and Oncology 2019;136:56–63. https://doi.org/10.1016/j.radonc.2019.03.026.
[49] Han X. MR-based synthetic CT generation using a deep convolutional neural network method. Med Phys 2017;44:1408–19. https://doi.org/10.1002/mp.12155.
[50] Lei Y, Harms J, Wang T, Liu Y, Shu H-K, Jani AB, et al. MRI-only based synthetic CT generation using dense cycle consistent generative adversarial networks. Medical Physics 2019;46:3565–81. https://doi.org/10.1002/mp.13617.
[51] Olberg S, Zhang H, Kennedy WR, Chun J, Rodriguez V, Zoberi I, et al. Synthetic CT reconstruction using a deep spatial pyramid convolutional framework for MR-only breast radiotherapy. Medical Physics 2019;46:4135–47. https://doi.org/10.1002/mp.13716.
[52] Dinkla AM, Florkow MC, Maspero M, Savenije MHF, Zijlstra F, Doornaert PAH, et al. Dosimetric evaluation of synthetic CT for head and neck radiotherapy generated by a patch-based three-dimensional convolutional neural network. Med Phys 2019;46:4095–104. https://doi.org/10.1002/mp.13663.
[53] Klages P, Benslimane I, Riyahi S, Jiang J, Hunt M, Deasy JO, et al. Patch-based generative adversarial neural network models for head and neck MR-only planning. Med Phys 2020;47:626–42. https://doi.org/10.1002/mp.13927.
[54] Qi M, Li Y, Wu A, Jia Q, Li B, Sun W, et al. Multi-sequence MR image-based synthetic CT generation using a generative adversarial network for head and neck MRI-only radiotherapy. Medical Physics 2020;47:1880–94. https://doi.org/10.1002/mp.14075.

[55] Tie X, Lam S-K, Zhang Y, Lee K-H, Au K-H, Cai J. Pseudo-CT generation from multi-parametric MRI using a novel multi-channel multi-path conditional generative adversarial network for nasopharyngeal carcinoma patients. Medical Physics 2020;47:1750–62. https://doi.org/10.1002/mp.14062.
[56] Wang Y, Liu C, Zhang X, Deng W. Synthetic CT Generation Based on T2 Weighted MRI of Nasopharyngeal Carcinoma (NPC) Using a Deep Convolutional Neural Network (DCNN). Frontiers in Oncology 2019;9. https://doi.org/10.3389/fonc.2019.01333.
[57] Florkow MC, Zijlstra F, Willemsen K, Maspero M, van den Berg CAT, Kerkmeijer LGW, et al. Deep learning–based MR-to-CT synthesis: The influence of varying gradient echo–based MR images as input channels. Magnetic Resonance in Medicine 2020;83:1429–41. https://doi.org/10.1002/mrm.28008.
[58] Fu J, Singhrao K, Cao M, Yu V, Santhanam AP, Yang Y, et al. Generation of abdominal synthetic CTs from 0.35T MR images using generative adversarial networks for MR-only liver radiotherapy. Biomedical Physics and Engineering Express 2020;6. https://doi.org/10.1088/2057-1976/ab6e1f.
[59] Liu L, Jolly S, Cao Y, Vineberg K, Fessler JA, Balter JM. Female pelvic synthetic CT generation based on joint intensity and shape analysis. Phys Med Biol 2017;62:2935–49. https://doi.org/10.1088/1361-6560/62/8/2935.
[60] Qian P, Xu K, Wang T, Zheng Q, Yang H, Baydoun A, et al. Estimating CT from MR Abdominal Images Using Novel Generative Adversarial Networks. Journal of Grid Computing 2020;18:211–26. https://doi.org/10.1007/s10723-020-09513-3.
[61] Xu K, Cao J, Xia K, Yang H, Zhu J, Wu C, et al. Multichannel Residual Conditional GAN-Leveraged Abdominal Pseudo-CT Generation via Dixon MR Images. IEEE Access 2019;7:163823–30. https://doi.org/10.1109/ACCESS.2019.2951924.
[62] Liu Y, Lei Y, Wang T, Kayode O, Tian S, Liu T, et al. MRI-based treatment planning for liver stereotactic body radiotherapy: Validation of a deep learning-based synthetic CT generation method. British Journal of Radiology 2019;92. https://doi.org/10.1259/bjr.20190067.
[63] Arabi H, Dowling JA, Burgos N, Han X, Greer PB, Koutsouvelis N, et al. Comparison of synthetic CT generation algorithms for MRI-only radiation planning in the pelvic region, 2018. https://doi.org/10.1109/NSSMIC.2018.8824321.
[64] Bahrami A, Karimian A, Fatemizadeh E, Arabi H, Zaidi H. A new deep convolutional neural network design with efficient learning capability: Application to CT image synthesis from MRI. Medical Physics 2020;47:5158–71. https://doi.org/10.1002/mp.14418.
[65] Leynes AP, Larson PEZ. Synthetic CT generation using MRI with deep learning: How does the selection of input images affect the resulting synthetic CT? vol. 2018- April, 2018, p. 6692–6. https://doi.org/10.1109/ICASSP.2018.8462419.
[66] Chen S, Qin A, Zhou D, Yan D. Technical Note: U-net-generated synthetic CT images for magnetic resonance imaging-only prostate intensity-modulated radiation therapy treatment planning. Medical Physics 2018;45:5659–65. https://doi.org/10.1002/mp.13247.
[67] Fu J, Yang Y, Singhrao K, Ruan D, Chu F-I, Low DA, et al. Deep learning approaches using 2D and 3D convolutional neural networks for generating male pelvic synthetic computed tomography from magnetic resonance imaging. Medical Physics 2019;46:3788–98. https://doi.org/10.1002/mp.13672.
[68] Bird D, Nix MG, McCallum H, Teo M, Gilbert A, Casanova N, et al. Multicentre, deep learning, synthetic-CT generation for ano-rectal MR-only radiotherapy treatment planning. Radiotherapy and Oncology 2021;156:23–8. https://doi.org/10.1016/j.radonc.2020.11.027.
[69] Sahiner B, Pezeshk A, Hadjiiski LM, Wang X, Drukker K, Cha KH, et al. Deep learning in medical imaging and radiation therapy. Med Phys 2019;46:e1–36. https://doi.org/10.1002/mp.13264.
[70] Bernal J, Kushibar K, Asfaw DS, Valverde S, Oliver A, Martí R, et al. Deep convolutional neural networks for brain image analysis on magnetic resonance imaging: a review. Artif Intell Med 2019;95:64–81. https://doi.org/10.1016/j.artmed.2018.08.008.
[71] Hesamian MH, Jia W, He X, Kennedy P. Deep Learning Techniques for Medical Image Segmentation: Achievements and Challenges. J Digit Imaging 2019;32:582–96. https://doi.org/10.1007/s10278-019-00227-x.
[72] Goodfellow IJ, Pouget-Abadie J, Mirza M, Xu B, Warde-Farley D, Ozair S, et al. Generative Adversarial Networks. ArXiv:14062661 [Cs, Stat] 2014.

[73] Ronneberger O, Fischer P, Brox T. U-Net: Convolutional Networks for Biomedical Image Segmentation. ArXiv:150504597 [Cs] 2015.
[74] Neppl S, Landry G, Kurz C, Hansen DC, Hoyle B, Stöcklein S, et al. Evaluation of proton and photon dose distributions recalculated on 2D and 3D Unet-generated pseudoCTs from T1-weighted MR head scans. Acta Oncologica 2019;58:1429–34. https://doi.org/10.1080/0284186X.2019.1630754.
[75] Maspero M, Bentvelzen LG, Savenije MHF, Guerreiro F, Seravalli E, Janssens GO, et al. Deep learning-based synthetic CT generation for paediatric brain MR-only photon and proton radiotherapy. Radiotherapy and Oncology 2020;153:197–204. https://doi.org/10.1016/j.radonc.2020.09.029.
[76] Bird D, Henry AM, Sebag-Montefiore D, Buckley DL, Al-Qaisieh B, Speight R. A Systematic Review of the Clinical Implementation of Pelvic Magnetic Resonance Imaging-Only Planning for External Beam Radiation Therapy. Int J Radiat Oncol Biol Phys 2019;105:479–92. https://doi.org/10.1016/j.ijrobp.2019.06.2530.
[77] Tenhunen M, Korhonen J, Kapanen M, Seppälä T, Koivula L, Collan J, et al. MRI-only based radiation therapy of prostate cancer: workflow and early clinical experience. Acta Oncol 2018;57:902–7. https://doi.org/10.1080/0284186X.2018.1445284.
[78] Florkow MC, Guerreiro F, Zijlstra F, Seravalli E, Janssens GO, Maduro JH, et al. Deep learning-enabled MRI-only photon and proton therapy treatment planning for paediatric abdominal tumours. Radiotherapy and Oncology 2020;153:220–7. https://doi.org/10.1016/j.radonc.2020.09.056.
[79] Largent A, Marage L, Gicquiau I, Nunes J-C, Reynaert N, Castelli J, et al. Head-and-Neck MRI-only radiotherapy treatment planning: From acquisition in treatment position to pseudo-CT generation. Cancer/Radiotherapie 2020;24:288–97. https://doi.org/10.1016/j.canrad.2020.01.008.
[80] Cardenas CE, Yang J, Anderson BM, Court LE, Brock KB. Advances in Auto-Segmentation. Semin Radiat Oncol 2019;29:185–97. https://doi.org/10.1016/j.semradonc.2019.02.001.
[81] González-Villà S, Oliver A, Valverde S, Wang L, Zwiggelaar R, Lladó X. A review on brain structures segmentation in magnetic resonance imaging. Artif Intell Med 2016;73:45–69. https://doi.org/10.1016/j.artmed.2016.09.001.
[82] Valentini V, Boldrini L, Damiani A, Muren LP. Recommendations on how to establish evidence from auto-segmentation software in radiotherapy. Radiother Oncol 2014;112:317–20. https://doi.org/10.1016/j.radonc.2014.09.014.
[83] Rigaud B, Simon A, Castelli J, Lafond C, Acosta O, Haigron P, et al. Deformable image registration for radiation therapy: principle, methods, applications and evaluation. Acta Oncol 2019;58:1225–37. https://doi.org/10.1080/0284186X.2019.1620331.
[84] Vrtovec T, Močnik D, Strojan P, Pernuš F, Ibragimov B. Auto-segmentation of organs at risk for head and neck radiotherapy planning: From atlas-based to deep learning methods. Med Phys 2020;47:e929–50. https://doi.org/10.1002/mp.14320.
[85] Zabel WJ, Conway JL, Gladwish A, Skliarenko J, Didiodato G, Goorts-Matthews L, et al. Clinical Evaluation of Deep Learning and Atlas-Based Auto-Contouring of Bladder and Rectum for Prostate Radiation Therapy. Pract Radiat Oncol 2021;11:e80–9. https://doi.org/10.1016/j.prro.2020.05.013.
[86] Lustberg T, van Soest J, Gooding M, Peressutti D, Aljabar P, van der Stoep J, et al. Clinical evaluation of atlas and deep learning based automatic contouring for lung cancer. Radiother Oncol 2018;126:312–7. https://doi.org/10.1016/j.radonc.2017.11.012.
[87] Fu Y, Mazur TR, Wu X, Liu S, Chang X, Lu Y, et al. A novel MRI segmentation method using CNN-based correction network for MRI-guided adaptive radiotherapy. Med Phys 2018;45:5129–37. https://doi.org/10.1002/mp.13221.
[88] Wang J, Lu J, Qin G, Shen L, Sun Y, Ying H, et al. Technical Note: A deep learning-based autosegmentation of rectal tumors in MR images. Med Phys 2018;45:2560–4. https://doi.org/10.1002/mp.12918.
[89] Taha AA, Hanbury A. Metrics for evaluating 3D medical image segmentation: analysis, selection, and tool. BMC Med Imaging 2015;15:29. https://doi.org/10.1186/s12880-015-0068-x.
[90] Yeghiazaryan V, Voiculescu I. Family of boundary overlap metrics for the evaluation of medical image segmentation. J Med Imaging (Bellingham) 2018;5:015006. https://doi.org/10.1117/1.JMI.5.1.015006.

[91] Meyer P, Noblet V, Mazzara C, Lallement A. Survey on deep learning for radiotherapy. Comput Biol Med 2018;98:126–46. https://doi.org/10.1016/j.compbiomed.2018.05.018.
[92] Litjens G, Kooi T, Bejnordi BE, Setio AAA, Ciompi F, Ghafoorian M, et al. A survey on deep learning in medical image analysis. Med Image Anal 2017;42:60–88. https://doi.org/10.1016/j.media.2017.07.005.
[93] Akkus Z, Galimzianova A, Hoogi A, Rubin DL, Erickson BJ. Deep Learning for Brain MRI Segmentation: State of the Art and Future Directions. J Digit Imaging 2017;30:449–59. https://doi.org/10.1007/s10278-017-9983-4.
[94] Russakovsky O, Deng J, Su H, Krause J, Satheesh S, Ma S, et al. ImageNet Large Scale Visual Recognition Challenge. Int J Comput Vis 2015;115:211–52. https://doi.org/10.1007/s11263-015-0816-y.
[95] Guo Y, Gao Y, Shen D. Deformable MR Prostate Segmentation via Deep Feature Learning and Sparse Patch Matching. IEEE Trans Med Imaging 2016;35:1077–89. https://doi.org/10.1109/TMI.2015.2508280.
[96] Feng Z, Nie D, Wang L, Shen D. SEMI-SUPERVISED LEARNING FOR PELVIC MR IMAGE SEGMENTATION BASED ON MULTI-TASK RESIDUAL FULLY CONVOLUTIONAL NETWORKS. Proc IEEE Int Symp Biomed Imaging 2018;2018:885–8. https://doi.org/10.1109/ISBI.2018.8363713.
[97] Elguindi S, Zelefsky MJ, Jiang J, Veeraraghavan H, Deasy JO, Hunt MA, et al. Deep learning-based auto-segmentation of targets and organs-at-risk for magnetic resonance imaging only planning of prostate radiotherapy. Phys Imaging Radiat Oncol 2019;12:80–6. https://doi.org/10.1016/j.phro.2019.11.006.
[98] Eppenhof K a. J, Maspero M, Savenije MHF, de Boer JCJ, van der Voort van Zyp JRN, Raaymakers BW, et al. Fast contour propagation for MR-guided prostate radiotherapy using convolutional neural networks. Med Phys 2020;47:1238–48. https://doi.org/10.1002/mp.13994.
[99] Savenije MHF, Maspero M, Sikkes GG, van der Voort van Zyp JRN, T J Kotte AN, Bol GH, et al. Clinical implementation of MRI-based organs-at-risk auto-segmentation with convolutional networks for prostate radiotherapy. Radiat Oncol 2020;15:104. https://doi.org/10.1186/s13014-020-01528-0.
[100] Kuisma A, Ranta I, Keyrilainen J, Suilamo S, Wright P, Pesola M, et al. Validation of automated magnetic resonance image segmentation for radiation therapy planning in prostate cancer. Physics and Imaging in Radiation Oncology 2020;13:14–20. https://doi.org/10.1016/j.phro.2020.02.004.
[101] Gou S, Lee P, Hu P, Rwigema J-C, Sheng K. Feasibility of automated 3-dimensional magnetic resonance imaging pancreas segmentation. Adv Radiat Oncol 2016;1:182–93. https://doi.org/10.1016/j.adro.2016.05.002.
[102] Liang Y, Schott D, Zhang Y, Wang Z, Nasief H, Paulson E, et al. Auto-segmentation of pancreatic tumor in multi-parametric MRI using deep convolutional neural networks. Radiother Oncol 2020;145:193–200. https://doi.org/10.1016/j.radonc.2020.01.021.
[103] Liang F, Qian P, Su K-H, Baydoun A, Leisser A, Van Hedent S, et al. Abdominal, multi-organ, auto-contouring method for online adaptive magnetic resonance guided radiotherapy: An intelligent, multi-level fusion approach. Artif Intell Med 2018;90:34–41. https://doi.org/10.1016/j.artmed.2018.07.001.
[104] Fu Y, Mazur TR, Wu X, Liu S, Chang X, Lu Y, et al. A novel MRI segmentation method using CNN-based correction network for MRI-guided adaptive radiotherapy. Med Phys 2018;45:5129–37. https://doi.org/10.1002/mp.13221.
[105] Chen Y, Ruan D, Xiao J, Wang L, Sun B, Saouaf R, et al. Fully automated multiorgan segmentation in abdominal magnetic resonance imaging with deep neural networks. Med Phys 2020;47:4971–82. https://doi.org/10.1002/mp.14429.
[106] Gurney-Champion OJ, Kieselmann JP, Wong KH, Ng-Cheng-Hin B, Harrington K, Oelfke U. A convolutional neural network for contouring metastatic lymph nodes on diffusion-weighted magnetic resonance images for assessment of radiotherapy response. Physics and Imaging in Radiation Oncology 2020;15:1–7. https://doi.org/10.1016/j.phro.2020.06.002.
[107] Lin L, Dou Q, Jin Y-M, Zhou G-Q, Tang Y-Q, Chen W-L, et al. Deep Learning for Automated Contouring of Primary Tumor Volumes by MRI for Nasopharyngeal Carcinoma. Radiology 2019;291:677–86. https://doi.org/10.1148/radiol.2019182012.

[108] Fiorino C, Gumina C, Passoni P, Palmisano A, Broggi S, Cattaneo GM, et al. A TCP-based early regression index predicts the pathological response in neo-adjuvant radio-chemotherapy of rectal cancer. Radiother Oncol 2018;128:564–8. https://doi.org/10.1016/j.radonc.2018.06.019.
[109] Castelli J, Simon A, Lafond C, Perichon N, Rigaud B, Chajon E, et al. Adaptive radiotherapy for head and neck cancer. Acta Oncol 2018;57:1284–92. https://doi.org/10.1080/0284186X.2018.1505053.
[110] Tanderup K, Lindegaard JC, Kirisits C, Haie-Meder C, Kirchheiner K, de Leeuw A, et al. Image Guided Adaptive Brachytherapy in cervix cancer: A new paradigm changing clinical practice and outcome. Radiother Oncol 2016;120:365–9. https://doi.org/10.1016/j.radonc.2016.08.007.
[111] van der Heide UA. MR-guided radiation therapy. Physica Medica 2016;32:175. https://doi.org/10.1016/j.ejmp.2016.07.284.
[112] Lambin P, Rios-Velazquez E, Leijenaar R, Carvalho S, van Stiphout RGPM, Granton P, et al. Radiomics: extracting more information from medical images using advanced feature analysis. Eur J Cancer 2012;48:441–6. https://doi.org/10.1016/j.ejca.2011.11.036.
[113] Lambin P, Leijenaar RTH, Deist TM, Peerlings J, de Jong EEC, van Timmeren J, et al. Radiomics: the bridge between medical imaging and personalized medicine. Nature Reviews Clinical Oncology 2017;14:749–62. https://doi.org/10.1038/nrclinonc.2017.141.
[114] Forghani R, Savadjiev P, Chatterjee A, Muthukrishnan N, Reinhold C, Forghani B. Radiomics and Artificial Intelligence for Biomarker and Prediction Model Development in Oncology. Comput Struct Biotechnol J 2019;17:995–1008. https://doi.org/10.1016/j.csbj.2019.07.001.
[115] Thorwarth D, Ege M, Nachbar M, Mönnich D, Gani C, Zips D, et al. Quantitative magnetic resonance imaging on hybrid magnetic resonance linear accelerators: Perspective on technical and clinical validation. Physics and Imaging in Radiation Oncology 2020;16:69–73. https://doi.org/10.1016/j.phro.2020.09.007.
[116] Cusumano D, Boldrini L, Yadav P, Casà C, Lee SL, Romano A, et al. Delta Radiomics Analysis for Local Control Prediction in Pancreatic Cancer Patients Treated Using Magnetic Resonance Guided Radiotherapy. Diagnostics 2021;11:72. https://doi.org/10.3390/diagnostics11010072.
[117] Boldrini L, Cusumano D, Chiloiro G, Casà C, Masciocchi C, Dinapoli N, et al. Delta Radiomics for rectal cancer response prediction with hybrid 0.35 T Magnetic Resonance guided Radiotherapy (MRgRT) : a hypothesis generating study for an innovative personalized medicine approach. La Radiologia Medica 2018.
[118] Jeon SH, Song C, Chie EK, Kim B, Kim YH, Chang W, et al. Delta-radiomics signature predicts treatment outcomes after preoperative chemoradiotherapy and surgery in rectal cancer. Radiat Oncol 2019;14:43. https://doi.org/10.1186/s13014-019-1246-8.
[119] Alahmari SS, Cherezov D, Goldgof D, Hall L, Gillies RJ, Schabath MB. Delta Radiomics Improves Pulmonary Nodule Malignancy Prediction in Lung Cancer Screening. IEEE Access 2018;6:77796–806. https://doi.org/10.1109/ACCESS.2018.2884126.
[120] Fave X, Zhang L, Yang J, Mackin D, Balter P, Gomez D, et al. Delta-radiomics features for the prediction of patient outcomes in non-small cell lung cancer. Sci Rep 2017;7:588. https://doi.org/10.1038/s41598-017-00665-z.
[121] Kumar V, Gu Y, Basu S, Berglund A, Eschrich SA, Schabath MB, et al. Radiomics: the process and the challenges. Magn Reson Imaging 2012;30:1234–48. https://doi.org/10.1016/j.mri.2012.06.010.
[122] Cusumano D, Dinapoli N, Boldrini L, Chiloiro G, Gatta R, Masciocchi C, et al. Fractal-based radiomic approach to predict complete pathological response after chemo-radiotherapy in rectal cancer. Radiol Med 2018;123:286–95. https://doi.org/10.1007/s11547-017-0838-3.
[123] Dinapoli N, Barbaro B, Gatta R, Chiloiro G, Casà C, Masciocchi C, et al. Magnetic Resonance, Vendor-independent, Intensity Histogram Analysis Predicting Pathologic Complete Response After Radiochemotherapy of Rectal Cancer. Int J Radiat Oncol Biol Phys 2018. https://doi.org/10.1016/j.ijrobp.2018.04.065.
[124] Wang J, Yung J, Kadbi M, Hwang K, Ding Y, Ibbott G. Assessment of image quality and scatter and leakage radiation of an integrated MR-LINAC system. Medical Physics 2018;45. https://doi.org/10.1002/mp.12767.

[125] Kooreman ES, van Houdt PJ, Nowee ME, van Pelt VWJ, Tijssen RHN, Paulson ES, et al. Feasibility and accuracy of quantitative imaging on a 1.5 T MR-linear accelerator. Radiother Oncol 2019;133:156–62. https://doi.org/10.1016/j.radonc.2019.01.011.
[126] Lorenz JW, Schott D, Rein L, Mostafaei F, Noid G, Lawton C, et al. Serial T2-Weighted Magnetic Resonance Images Acquired on a 1.5 Tesla Magnetic Resonance Linear Accelerator Reveal Radiomic Feature Variation in Organs at Risk: An Exploratory Analysis of Novel Metrics of Tissue Response in Prostate Cancer. Cureus 2019;11:e4510. https://doi.org/10.7759/cureus.4510.
[127] Cusumano D, Meijer G, Lenkowicz J, Chiloiro G, Boldrini L, Masciocchi C, et al. A field strength independent MR radiomics model to predict pathological complete response in locally advanced rectal cancer. Radiol Med 2020. https://doi.org/10.1007/s11547-020-01266-z.
[128] Simpson G, Spieler B, Dogan N, Portelance L, Mellon EA, Kwon D, et al. Predictive value of 0.35 T magnetic resonance imaging radiomic features in stereotactic ablative body radiotherapy of pancreatic cancer: A pilot study. Med Phys 2020;47:3682–90. https://doi.org/10.1002/mp.14200.
[129] Yang Y, Cao M, Sheng K, Gao Y, Chen A, Kamrava M, et al. Longitudinal diffusion MRI for treatment response assessment: Preliminary experience using an MRI-guided tri-cobalt 60 radiotherapy system. Med Phys 2016;43:1369–73. https://doi.org/10.1118/1.4942381.
[130] Cusumano D, Boldrini L, Yadav P, Gao Y, Chiloiro G, Musurunu B, et al. Delta radiomics for rectal cancer response prediction using low field magnetic resonance guided radiotherapy: an external validation. Phys Med 2021.
[131] Gao Y, Kalbasi A, Hsu W, Ruan D, Fu J, Shao J, et al. Treatment effect prediction for sarcoma patients treated with preoperative radiotherapy using radiomics features from longitudinal diffusion-weighted MRIs. Physics in Medicine and Biology 2020;65. https://doi.org/10.1088/1361-6560/ab9e58.
[132] Broggi S, Passoni P, Gumina C, Palmisano A, Bresolin A, Burgio V, et al. Predicting pathological response after radio-chemotherapy for rectal cancer: Impact of late oxaliplatin administration. Radiother Oncol 2020;149:174–80. https://doi.org/10.1016/j.radonc.2020.05.019.
[133] Cusumano D, Boldrini L, Yadav P, Yu G, Musurunu B, Chiloiro G, et al. External Validation of Early Regression Index (ERITCP) as Predictor of Pathologic Complete Response in Rectal Cancer Using Magnetic Resonance-Guided Radiation Therapy. Int J Radiat Oncol Biol Phys 2020;108:1347–56. https://doi.org/10.1016/j.ijrobp.2020.07.2323.
[134] Cusumano D, Catucci F, Romano A, Boldrini L, Piras A, Broggi S, et al. Evaluation of an Early Regression Index (ERITCP) as Predictor of Pathological Complete Response in Cervical Cancer: A Pilot-Study. Applied Sciences 2020;10:8001. https://doi.org/10.3390/app10228001.
[135] Cusumano D, Dhont J, Boldrini L, Chiloiro G, Teodoli S, Massaccesi M, et al. Predicting tumour motion during the whole radiotherapy treatment: a systematic approach for thoracic and abdominal lesions based on real time MR. Radiother Oncol 2018;129:456–62. https://doi.org/10.1016/j.radonc.2018.07.025.
[136] Dhont J, Vandemeulebroucke J, Burghelea M, Poels K, Depuydt T, Van Den Begin R, et al. The long- and short-term variability of breathing induced tumor motion in lung and liver over the course of a radiotherapy treatment. Radiother Oncol 2018;126:339–46. https://doi.org/10.1016/j.radonc.2017.09.001.
[137] Klüter S. Technical design and concept of a 0.35 T MR-Linac. Clin Transl Radiat Oncol 2019;18:98–101. https://doi.org/10.1016/j.ctro.2019.04.007.
[138] Paganelli C, Whelan B, Peroni M, Summers P, Fast M, van de Lindt T, et al. MRI-guidance for motion management in external beam radiotherapy: current status and future challenges. Phys Med Biol 2018;63:22TR03. https://doi.org/10.1088/1361-6560/aaebcf.
[139] Cerviño LI, Du J, Jiang SB. MRI-guided tumor tracking in lung cancer radiotherapy. Physics in Medicine and Biology 2011;56:3773–85. https://doi.org/10.1088/0031-9155/56/13/003.
[140] Yun J, Yip E, Gabos Z, Wachowicz K, Rathee S, Fallone BG. Neural-network based autocontouring algorithm for intrafractional lung-tumor tracking using Linac-MR. Medical Physics 2015;42:2296–310. https://doi.org/10.1118/1.4916657.

[141] Fast MF, Eiben B, Menten MJ, Wetscherek A, Hawkes DJ, McClelland JR, et al. Tumour auto-contouring on 2d cine MRI for locally advanced lung cancer: A comparative study. Radiotherapy and Oncology 2017;125:485–91. https://doi.org/10.1016/j.radonc.2017.09.013.
[142] Bourque AE, Carrier J-F, Filion É, Bedwani S. A particle filter motion prediction algorithm based on an autoregressive model for real-time MRI-guided radiotherapy of lung cancer. Biomed Phys Eng Express 2017;3:035001. https://doi.org/10.1088/2057-1976/aa6b5b.
[143] Mirzapour SA, Mazur T, Sharp G, Salari E. Intra-fraction motion prediction in MRI-guided radiation therapy using Markov processes. Phys Med Biol 2019;64:195006. https://doi.org/10.1088/1361-6560/ab37a9.
[144] Dhont J, Vandemeulebroucke J, Cusumano D, Boldrini L, Cellini F, Valentini V, et al. Multi-object tracking in MRI-guided radiotherapy using the tracking-learning-detection framework. Radiother Oncol 2019;138:25–9. https://doi.org/10.1016/j.radonc.2019.05.008.
[145] Kalal Z, Mikolajczyk K, Matas J. Tracking-Learning-Detection. IEEE Trans Pattern Anal Mach Intell 2012;34:1409–22. https://doi.org/10.1109/TPAMI.2011.239.
[146] Terpstra ML, Maspero M, d'Agata F, Stemkens B, Intven MPW, Lagendijk JJW, et al. Deep learning-based image reconstruction and motion estimation from undersampled radial k-space for real-time MRI-guided radiotherapy. Phys Med Biol 2020;65:155015. https://doi.org/10.1088/1361-6560/ab9358.
[147] Ghodrati V, Bydder M, Ali F, Gao C, Prosper A, Nguyen K-L, et al. Retrospective respiratory motion correction in cardiac cine MRI reconstruction using adversarial autoencoder and unsupervised learning. NMR Biomed 2020:e4433. https://doi.org/10.1002/nbm.4433.
[148] El-Rewaidy H, Fahmy AS, Pashakhanloo F, Cai X, Kucukseymen S, Csecs I, et al. Multi-domain convolutional neural network (MD-CNN) for radial reconstruction of dynamic cardiac MRI. Magn Reson Med 2021;85:1195–208. https://doi.org/10.1002/mrm.28485.
[149] Zhou J, Peng Z, Song Y, Chang Y, Pei X, Sheng L, et al. A method of using deep learning to predict three-dimensional dose distributions for intensity-modulated radiotherapy of rectal cancer. J Appl Clin Med Phys 2020;21:26–37. https://doi.org/10.1002/acm2.12849.
[150] Qin C, Schlemper J, Caballero J, Price AN, Hajnal JV, Rueckert D. Convolutional Recurrent Neural Networks for Dynamic MR Image Reconstruction. IEEE Transactions on Medical Imaging 2019;38:280–90. https://doi.org/10.1109/TMI.2018.2863670.
[151] Ke Z, Cheng J, Ying L, Zheng H, Zhu Y, Liang D. An unsupervised deep learning method for multi-coil cine MRI. Phys Med Biol 2020;65:235041. https://doi.org/10.1088/1361-6560/abaffa.
[152] Ghodrati V, Shao J, Bydder M, Zhou Z, Yin W, Nguyen K-L, et al. MR image reconstruction using deep learning: evaluation of network structure and loss functions. Quant Imaging Med Surg 2019;9:1516–27. https://doi.org/10.21037/qims.2019.08.10.
[153] Seppenwoolde Y, Shirato H, Kitamura K, Shimizu S, van Herk M, Lebesque JV, et al. Precise and real-time measurement of 3D tumor motion in lung due to breathing and heartbeat, measured during radiotherapy. Int J Radiat Oncol Biol Phys 2002;53:822–34. https://doi.org/10.1016/s0360-3016(02)02803-1.
[154] Küstner T, Fuin N, Hammernik K, Bustin A, Qi H, Hajhosseiny R, et al. CINENet: deep learning-based 3D cardiac CINE MRI reconstruction with multi-coil complex-valued 4D spatio-temporal convolutions. Sci Rep 2020;10:13710. https://doi.org/10.1038/s41598-020-70551-8.
[155] Stemkens B, Tijssen RHN, de Senneville BD, Lagendijk JJW, van den Berg CAT. Image-driven, model-based 3D abdominal motion estimation for MR-guided radiotherapy. Phys Med Biol 2016;61:5335–55. https://doi.org/10.1088/0031-9155/61/14/5335.
[156] Harris W, Ren L, Cai J, Zhang Y, Chang Z, Yin F-F. A Technique for Generating Volumetric Cine-Magnetic Resonance Imaging. Int J Radiat Oncol Biol Phys 2016;95:844–53. https://doi.org/10.1016/j.ijrobp.2016.02.011.
[157] Rabe M, Paganelli C, Riboldi M, Bondesson D, Schneider MJ, Chmielewski T, et al. Porcine lung phantom-based validation of estimated 4D-MRI using orthogonal cine imaging for low-field MR-Linacs. Phys Med Biol 2020. https://doi.org/10.1088/1361-6560/abc937.

[158] Paganelli C, Portoso S, Garau N, Meschini G, Via R, Buizza G, et al. Time-resolved volumetric MRI in MRI-guided radiotherapy: an in silico comparative analysis. Phys Med Biol 2019;64:185013. https://doi.org/10.1088/1361-6560/ab33e5.
[159] McClelland JR, Modat M, Arridge S, Grimes H, D'Souza D, Thomas D, et al. A generalized framework unifying image registration and respiratory motion models and incorporating image reconstruction, for partial image data or full images. Phys Med Biol 2017;62:4273–92. https://doi.org/10.1088/1361-6560/aa6070.
[160] Tran EH, Eiben B, Wetscherek A, Oelfke U, Meedt G, Hawkes DJ, et al. Evaluation of MRI-derived surrogate signals to model respiratory motion. Biomed Phys Eng Express 2020;6:045015. https://doi.org/10.1088/2057-1976/ab944c.
[161] Ginn J, Lamb J, Ruan D. Online target volume estimation and prediction from an interlaced slice acquisition - A manifold embedding and learning approach. Lecture Notes in Computer Science (Including Subseries Lecture Notes in Artificial Intelligence and Lecture Notes in Bioinformatics) 2019;11850 LNCS:78–85. https://doi.org/10.1007/978-3-030-32486-5_10.
[162] Ginn JS, Ruan D, Low DA, Lamb JM. Multislice motion modeling for MRI-guided radiotherapy gating. Med Phys 2019;46:465–74. https://doi.org/10.1002/mp.13350.
[163] Kissick MW, Mackie TR. Task Group 76 Report on 'The management of respiratory motion in radiation oncology' [Med. Phys. 33, 3874–3900 (2006)]. Med Phys 2009;36:5721–2. https://doi.org/10.1118/1.3260838.
[164] Kim T, Park JC, Gach HM, Chun J, Mutic S. Technical Note: Real-time 3D MRI in the presence of motion for MRI-guided radiotherapy: 3D Dynamic keyhole imaging with super-resolution. Medical Physics 2019;46:4631–8. https://doi.org/10.1002/mp.13748.
[165] Zhao C, Shao M, Carass A, Li H, Dewey BE, Ellingsen LM, et al. Applications of a deep learning method for anti-aliasing and super-resolution in MRI. Magn Reson Imaging 2019;64:132–41. https://doi.org/10.1016/j.mri.2019.05.038.
[166] Wang et al. Artificial Intelligence in Radiotherapy Treatment Planning: Present and Future 2019.
[167] Hussein M, Heijmen BJM, Verellen D, Nisbet A. Automation in intensity modulated radiotherapy treatment planning—a review of recent innovations. BJR 2018;91:20180270. https://doi.org/10.1259/bjr.20180270.
[168] EthosTM therapy AI Technical Brief 2019.
[169] Moore KL. Automated Radiotherapy Treatment Planning. Semin Radiat Oncol 2019;29:209–18. https://doi.org/10.1016/j.semradonc.2019.02.003.
[170] Cagni E, Botti A, Micera R, Galeandro M, Sghedoni R, Orlandi M, et al. Knowledge-based treatment planning: An inter-technique and inter-system feasibility study for prostate cancer. Phys Med 2017;36:38–45. https://doi.org/10.1016/j.ejmp.2017.03.002.
[171] Rago M, Placidi L, Polsoni M, Rambaldi G, Cusumano D, Greco F, et al. Evaluation of a generalized knowledge-based planning performance for VMAT irradiation of breast and locoregional lymph nodes-Internal mammary and/or supraclavicular regions. PLoS One 2021;16:e0245305. https://doi.org/10.1371/journal.pone.0245305.
[172] Teichert K, Süss P, Serna JI, Monz M, Küfer KH, Thieke C. Comparative analysis of Pareto surfaces in multi-criteria IMRT planning. Phys Med Biol 2011;56:3669–84. https://doi.org/10.1088/0031-9155/56/12/014.
[173] Breedveld S, Storchi PRM, Keijzer M, Heemink AW, Heijmen BJM. A novel approach to multi-criteria inverse planning for IMRT. Phys Med Biol 2007;52:6339–53. https://doi.org/10.1088/0031-9155/52/20/016.
[174] Bijman R, Rossi L, Janssen T, de Ruiter P, Carbaat C, van Triest B, et al. First system for fully-automated multi-criterial treatment planning for a high-magnetic field MR-Linac applied to rectal cancer. Acta Oncologica 2020;59:926–32. https://doi.org/10.1080/0284186X.2020.1766697.
[175] Wang M, Zhang Q, Lam S, Cai J, Yang R. A Review on Application of Deep Learning Algorithms in External Beam Radiotherapy Automated Treatment Planning. Front Oncol 2020;10:580919. https://doi.org/10.3389/fonc.2020.580919.

[176] Shen C, Nguyen D, Chen L, Gonzalez Y, McBeth R, Qin N, et al. Operating a treatment planning system using a deep-reinforcement learning-based virtual treatment planner for prostate cancer intensity-modulated radiation therapy treatment planning. Med Phys 2020;47:2329–36. https://doi.org/10.1002/mp.14114.
[177] Castriconi R, Fiorino C, Passoni P, Broggi S, Di Muzio NG, Cattaneo GM, et al. Knowledge-based automatic optimization of adaptive early-regression-guided VMAT for rectal cancer. Physica Medica 2020;70:58–64. https://doi.org/10.1016/j.ejmp.2020.01.016.
[178] Placidi L, Lenkowicz J, Cusumano D, Boldrini L, Dinapoli N, Valentini V. Stability of dosomics features extraction on grid resolution and algorithm for radiotherapy dose calculation. Phys Med 2020;77:30–5. https://doi.org/10.1016/j.ejmp.2020.07.022.
[179] Scott JG, Berglund A, Schell MJ, Mihaylov I, Fulp WJ, Yue B, et al. A genome-based model for adjusting radiotherapy dose (GARD): a retrospective, cohort-based study. Lancet Oncol 2017;18:202–11. https://doi.org/10.1016/S1470-2045(16)30648-9.
[180] Li HH, Rodriguez VL, Green OL, Hu Y, Kashani R, Wooten HO, et al. Patient-specific quality assurance for the delivery of (60)Co intensity modulated radiation therapy subject to a 0.35-T lateral magnetic field. Int J Radiat Oncol Biol Phys 2015;91:65–72. https://doi.org/10.1016/j.ijrobp.2014.09.008.
[181] Chen X, Ahunbay E, Paulson E, Chen G, Li X. A daily end-to-end quality assurance workflow for MR-guided online adaptive radiation therapy on MR-Linac: Daily end-to-end QA workflow for MR-Linac. Journal of Applied Clinical Medical Physics 2019;21. https://doi.org/10.1002/acm2.12786.
[182] Madden L, Archer J, Li E, Jelen U, Dong B, Roberts N, et al. First measurements with a plastic scintillation dosimeter at the Australian MRI-LINAC. Phys Med Biol 2019;64:175015. https://doi.org/10.1088/1361-6560/ab324b.
[183] Cusumano D, Placidi L, D'Agostino E, Boldrini L, Menna S, Valentini V, et al. Characterization of an inorganic scintillator for small-field dosimetry in MR-guided radiotherapy. J Appl Clin Med Phys 2020;21:244–51. https://doi.org/10.1002/acm2.13012.
[184] McNutt TR, Moore KL, Wu B, Wright JL. Use of Big Data for Quality Assurance in Radiation Therapy. Semin Radiat Oncol 2019;29:326–32. https://doi.org/10.1016/j.semradonc.2019.05.006.
[185] Kalet AM, Gennari JH, Ford EC, Phillips MH. Bayesian network models for error detection in radiotherapy plans. Phys Med Biol 2015;60:2735–49. https://doi.org/10.1088/0031-9155/60/7/2735.
[186] Tol JP, Dahele M, Delaney AR, Slotman BJ, Verbakel WFAR. Can knowledge-based DVH predictions be used for automated, individualized quality assurance of radiotherapy treatment plans? Radiat Oncol 2015;10:234. https://doi.org/10.1186/s13014-015-0542-1.
[187] Nguyen D, Long T, Jia X, Lu W, Gu X, Iqbal Z, et al. A feasibility study for predicting optimal radiation therapy dose distributions of prostate cancer patients from patient anatomy using deep learning. Sci Rep 2019;9:1076. https://doi.org/10.1038/s41598-018-37741-x.
[188] Valdes G, Scheuermann R, Hung CY, Olszanski A, Bellerive M, Solberg TD. A mathematical framework for virtual IMRT QA using machine learning. Med Phys 2016;43:4323. https://doi.org/10.1118/1.4953835.
[189] Valdes G, Chan MF, Lim SB, Scheuermann R, Deasy JO, Solberg TD. IMRT QA using machine learning: A multi-institutional validation. J Appl Clin Med Phys 2017;18:279–84. https://doi.org/10.1002/acm2.12161.
[190] Lam D, Zhang X, Li H, Deshan Y, Schott B, Zhao T, et al. Predicting gamma passing rates for portal dosimetry-based IMRT QA using machine learning. Med Phys 2019;46:4666–75. https://doi.org/10.1002/mp.13752.
[191] Li J, Wang L, Zhang X, Liu L, Li J, Chan MF, et al. Machine Learning for Patient-Specific Quality Assurance of VMAT: Prediction and Classification Accuracy. Int J Radiat Oncol Biol Phys 2019;105:893–902. https://doi.org/10.1016/j.ijrobp.2019.07.049.
[192] Tomori S, Kadoya N, Takayama Y, Kajikawa T, Shima K, Narazaki K, et al. A deep learning-based prediction model for gamma evaluation in patient-specific quality assurance. Med Phys 2018. https://doi.org/10.1002/mp.13112.

[193] Mahdavi SR, Tavakol A, Sanei M, Molana SH, Arbabi F, Rostami A, et al. Use of artificial neural network for pretreatment verification of intensity modulation radiation therapy fields. Br J Radiol 2019;92:20190355. https://doi.org/10.1259/bjr.20190355.
[194] Kimura Y, Kadoya N, Tomori S, Oku Y, Jingu K. Error detection using a convolutional neural network with dose difference maps in patient-specific quality assurance for volumetric modulated arc therapy. Phys Med 2020;73:57–64. https://doi.org/10.1016/j.ejmp.2020.03.022.
[195] Interian Y, Rideout V, Kearney VP, Gennatas E, Morin O, Cheung J, et al. Deep nets vs expert designed features in medical physics: An IMRT QA case study. Med Phys 2018;45:2672–80. https://doi.org/10.1002/mp.12890.
[196] Cusumano D, Dhont J, Boldrini L, Chiloiro G, Romano A, Votta C, et al. Reliability of ITV approach to varying treatment fraction time: a retrospective analysis based on 2D cine MR images. Radiat Oncol 2020;15:152. https://doi.org/10.1186/s13014-020-01530-6.
[197] van Sörnsen de Koste JR, Palacios MA, Bruynzeel AME, Slotman BJ, Senan S, Lagerwaard FJ. MR-guided Gated Stereotactic Radiation Therapy Delivery for Lung, Adrenal, and Pancreatic Tumors: A Geometric Analysis. Int J Radiat Oncol Biol Phys 2018;102:858–66. https://doi.org/10.1016/j.ijrobp.2018.05.048.
[198] Brouwer CL, Dinkla AM, Vandewinckele L, Crijns W, Claessens M, Verellen D, et al. Machine learning applications in radiation oncology: Current use and needs to support clinical implementation. Phys Imaging Radiat Oncol 2020;16:144–8. https://doi.org/10.1016/j.phro.2020.11.002.
[199] Keskinbora KH. Medical ethics considerations on artificial intelligence. J Clin Neurosci 2019;64:277–82. https://doi.org/10.1016/j.jocn.2019.03.001.